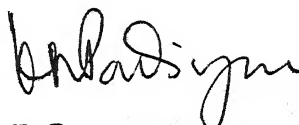# SIMULATION OF HV DC LINK FOR CONTROL AND STABILITY STUDIES

By

V. VENKATESWAR RAO

EE-1978-M-RAE-SIM

## CERTIFICATE

Certified that the work entitled "Simulation of HVDC Link for Control and Stability Studies" by Mr. V. Venkateswar Rao has been carried out under my supervision and has not been submitted elsewhere for the award of a degree.

K.R. Padiyar
Assistant Professor
Department of Electrical Engineering
Indian Institute of Technology
Kanpur

July 1978.

## ACKNOWLEDGEMENTS

# TABLE OF CONTENTS

CHAPTER 5 :   DIGITAL SIMULATION OF A PARALLEL
              AC/DC SYSTEM

# ABSTRACT

The application of HVDC transmission has been
increasing in the recent years because of certain technical
advantages associated with it.  These include (i) Elimination
of reactive power requirements of the line which makes it
attractive for underground cables (2) Elimination of
stability problem associated with long distance transmission
as the DC link is essentially asynchronous link and (3) No
increase in the short circuit level because of fast acting
controls. DC transmission is also economical over the AC
transmission over long distances and has proved to be
reliable in operation.

The control system  of the DC link has an important
effect on the performance of the DC link.  The first problem
of this thesis deals with the simulation of HVDC link and
its controls, and the study of the effects of the controls
when the DC link is subjected to change in reference power
and disturbances in AC voltages at both the rectifier
and inverter end.

The other interesting feature of the HVDC link is
the stabilization of AC system to which it is connected. It
was first suggested by Uhlmann in 1964 that by deriving
suitable control signals from the AC system the power
transferred through the DC link can be modulated and thus

the dynamic stability of the AC system can be improved. The second problem deals with the simulation of a two machine system with parallel AC/DC links and to investigate the stabilizing property of the DC link through adequate auxiliary controller.

# CHAPTER 1

## INTRODUCTION

### 1.1 GENERAL

High voltage direct current transmission has established itself as a well-proven transmission medium over more than two decades. Starting from the Gotland [1] project in Sweden which was commissioned in the year 1954, there are now about 23 projects in operation or under construction throughout the world. In early years it was thought that its essential use would lie in long distance bulk power transmission and much discussion centered on establishing a break-even distance beyond which HVDC would be cheaper than AC because the lower cost of lines and cables more than compensated for the higher cost of terminal equipment. Experience has, however, shown that other features such as the stabilization of AC link by DC link, the merits of which are now better appreciated, can lead the DC transmission to be a better alternative to AC transmission.

### 1.2 FACTORS CONTRIBUTING TO INCREASED APPLICATION OF DC TRANSMISSION [2]

(i) Reliability: Experience with HVDC system in operation, especially the performance of the modern schemes using solid state valves, has given planners confidence in

the reliability of HVDC system. Overall availability of the first all solid-state terminal, the EEL River Project was better than 97 percent in 1975 and 76. The reliability performance of transmission lines has also been increasing.

(ii) Economic competitiveness: In long distance transmission where the choice of AC or DC is dictated by the total cost of the transmission facility, the basic economic considerations are well known: line costs are higher for AC and terminal costs are higher for DC; so if the line is long enough to give sufficient savings in line costs to offset the higher terminal costs, DC provides a more economical solution. In recent years, line costs for both AC and DC have been going up significantly while there has been little increase in DC terminal costs. With increased line costs for both AC and DC, the savings in line costs for DC also increases without an offsetting increase in terminal costs. In this situation DC becomes more attractive for shorter distances of transmission.

(iii) Stability considerations: Absence of conventional power system stability problems is a major advantage of DC interconnections. The DC link provides power coupling between two AC systems without sacrificing the autonomy of each system with regard to frequency changes. Often additional benefits can be obtained by using the controllability of power on the DC link to enhance the stability of connected AC systems.

In fact, the stabilization of AC link by a DC link is the most promising current area of research.

(iv) Control of short circuit levels: For AC systems with high short circuit levels, DC provides a means of expansion without further raising short circuit levels to the point of upgrading existing breakers.

HVDC transmission has many advantages and some disadvantages which can be summarized as follows: [3,4]

Advantages: (i)   Greater power per conductor

(ii)  Simpler line construction

(iii) Ground return can be used

(iv)  No charging effect

(v)   No skin effect

(vi)  Very fast response

(vii) Less corona loss and radio interference

(viii) Asynchronous linking

(ix)  Improvement of stability of AC system by the DC link

(x)   The short circuit level of the systems are not increased.

(xi)  No inherent instability and no need for intermediate switching stations

(xii) Each DC pole is independently controllable.

Disadvantages:

(i)   Terminal equipment are costly

(ii)  Harmonic distortion

(iii) Overload capacity is limited

(iv) Dependency on AC systems

(v) Rectifiers and inverters absorb reactive power and this must be supplied locally.

(vi) The possibility of interrupting circuit at current zero is absent in DC system. Because of this the switching has to be carried on AC side of the converter equipment. The lack of DC circuit breakers has restsicted the use of DC to only point to point transmission. However the development of DC circuit breakers is being carried and the availability of a reliable and economic breaker should lead to the introduction of multiterminal DC links.

## 1.3 ESSENTIAL FEATURES OF A HVDC TRANSMISSION SYSTEM

Fig.1.1 shows the schematic diagram of a 6 pulse bipolar HVDC transmission system. Bridge A operates as a rectifier to convert AC power to DC and bridge B operates as an inverter to convert the DC power back to AC.

The major equipment on a HVDC converter terminal are (i) Converter and its controls(ii) Converter transformer (iii) Smoothing reactor and (iv) AC filters which are shown in figure.
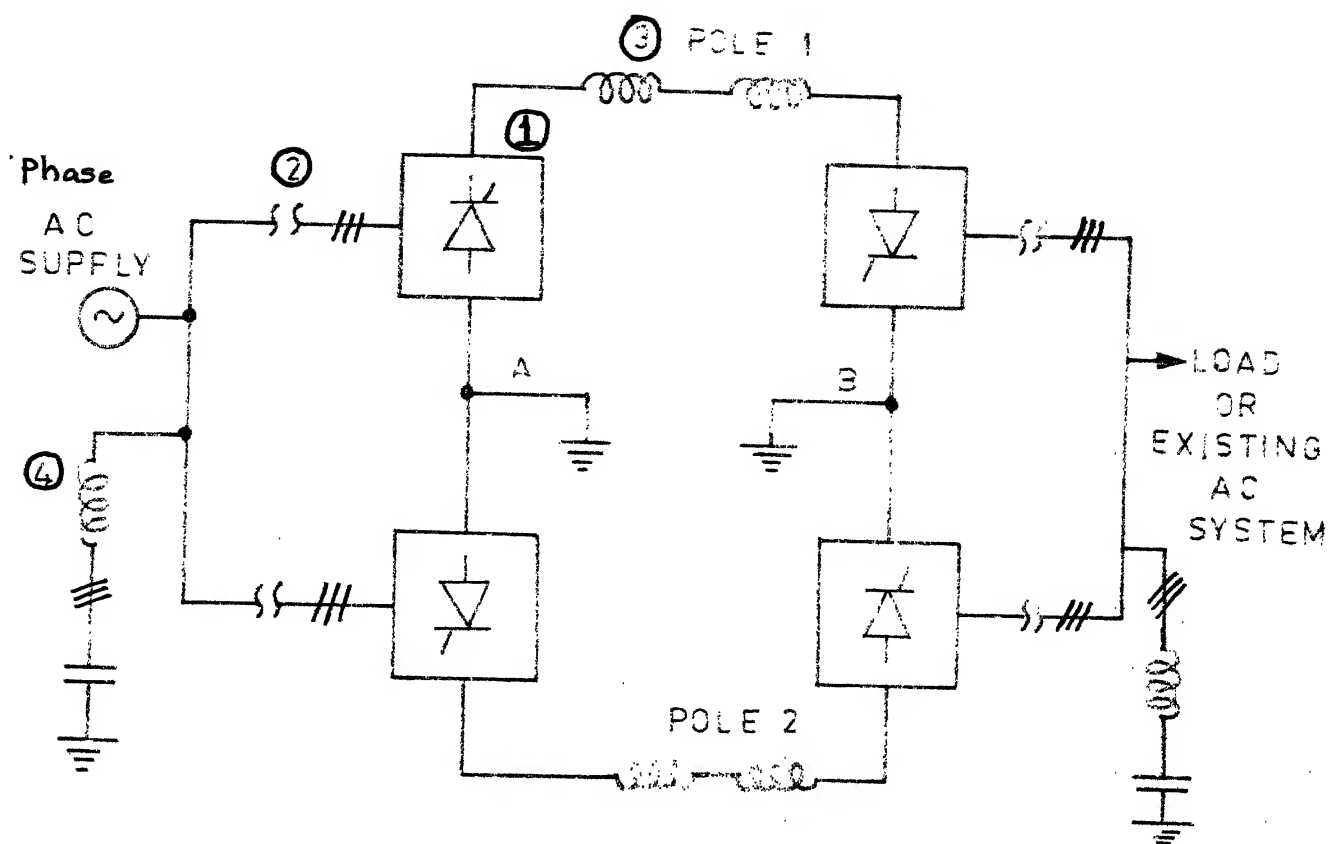
FIG.1.1 HVDC TRANSMISSION SYSTEM.
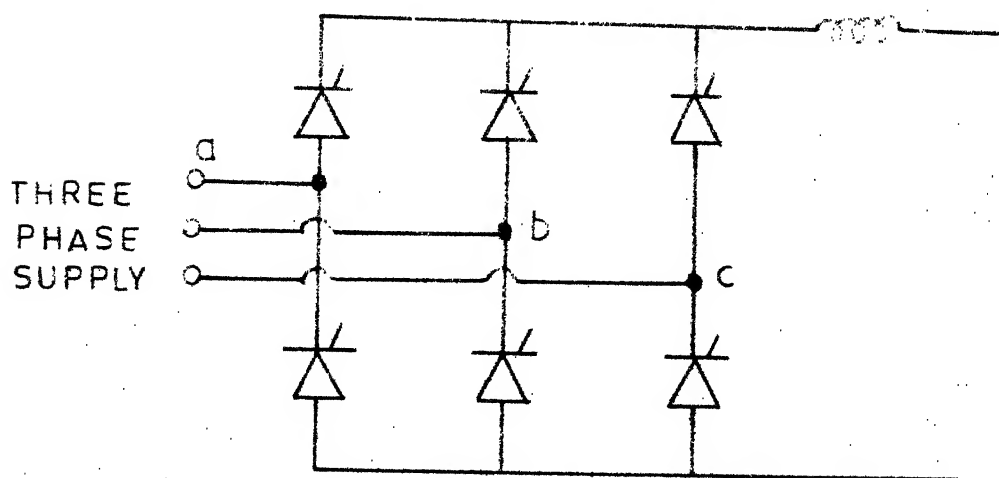


FIG.1.2 BRIDGE CONVERTER.

The detailed diagram of a 3-phase fully controlled, 6 pulse bridge converter is shown in Figure 1.2. The six valves are fired in sequence by control pulses at intervals of 60° electrical to obtain required operation. In every arm of a bridge a number of SCRs can be connected in series or parallel to obtain high ratings for current and voltage. Voltage and current equalising circuits and snubbers for protection of SCR's are used which are not shown in figure.

To reduce the ripple in the DC outputs and also the harmonics in the AC side, two such six pulse converters, one with an input transformer having star-star connection and the other with the input transformer, having star-delta connection, are used on each side of the DC link. This results in a twelve pulse operation which is invariably used with thyristor converters.

Smoothing reactors smoothen out the DC output of a converter and to limit the rate of rise of fault current in the event of a short circuit on the DC line.

To limit the amplitude of harmonics entering the AC network and the DC line, AC filters are used.

By controlling the firing angles of the valves in both rectifier and inverter, the current and the voltage in the DC link can be controlled.

## 1.4 SPECIAL EQUIPMENT

HVDC is a continuously evolving application and
has resulted in the development of much special equipment [5].

(i) Converter valves:  Upto about seven years ago all
schemes used mercury arc converter valves and after some
early problems these achieved a great degree of reliability.
The type ARBJ6 valves on the Nelson river scheme are the
world's largest and highest voltage units of any kind and
seem likely to remain so far for some years yet.  Although
some development was possible, the advances in semiconductor
techniques, particularly the voltage and current ratings of
thyristor devices, brought the thyristor valve into the
range of practical economics and it is presently the
accepted conversion medium.  Standard sizes and ratings of
mercury arc valves established the six pulse bridge group
as the normal building blocks for the HVDC schemes.  The
greater flexibility of rating, inherent in grouping of
thyristors has encouraged the adoption of 12 pulse pair
of bridges as the norm, which can be put together in series
or parallel to meet power requirements.

(ii) Control systems:  Control systems for HVDC links
have been designed using AC/DC simulators.  Simulator studies
predicted difficulties of operating converters in which the
Individual Phase Control systems (IPC) were used for grid control, o
relatively weak (high impedance) AC systems due to inherent

harmonic instability caused by distortion of the AC line
voltage supplying the controls. The problem was first
identified by Ainsworth and led to the introduction of the
phase locked oscillator control system which derived the
pulsing signal from an independent voltage controlled
oscillator circuit; this provided accurate and equidistant
converter timing pulses unaffected by the system load
conditions and was a significant step in the control of
HVDC schemes.

(iii) Converter transformers: The basic unit is the
three-phase six pulse transformer group, but it is now customary
to operate and switch these in 12 pulse pairs with alternate
star and delta windings.

(iv) Harmonic filters: In earlier schemes using mercury
arc valves, the economic size of the valve made a 12 pulse
converter too large a component for its sudden loss to be
tolerated by the system in which it is operated. Filters
were therefore designed to take account of converter
operation unbalanced by the loss of a six-pulse group. This
involved tuned AC filter banks to deal with 5th, 7th, 11th
and 13th harmonics and a high pass filter. Special attention
towards maintaining accuracy of tuning under varying frequency
and temperature conditions resulted in the adoption of the
automatically variable element in the component of the filter
bank. With the advent of the 12 pulse thyristor converter

assembly and a trend towards acceptance of sudden loss of larger blocks of power, filter designs now cater for 11th and 13th harmonics only and are smaller and cheaper.

## 1.5 STATEMENT OF THE PROBLEM

(i) During unbalanced conditions the **dynamic** performance of HVDC transmission systems connected to weak AC systems depends strongly upon the control system of the DC link. There has been much progress in developing new control systems to meet the demands of the expanding HVDC transmission links. And in the past, HVDC simulator was used to study the response of different types of converter control systems. However, similar simulation can be attempted on digital computer also.

The first problem that is considered in this thesis deals with the Digital simulation of HVDC transmission system and its controls in detail. The converter controls considered are typical of those used in the latest installations with thyristor valves. The purpose of this study is to simulate the response of the controller and the DC link subjected to disturbances in AC voltages and reference power. The AC system is not represented in detail.

(ii) Because of its ease of control, a HVDC transmission system can be used to influence the stability of associated AC networks. To improve stability, appropriate signals derived from the AC network are fed to the HVDC control system.

In view of this principle, an attempt has been made to investigate the manner in which a HVDC system, with and without the controller influences the transient stability of an AC network. A simplified DC link representation is used as this is considered adequate for the simulation of slow electromechanical transients.

The chapterwise description of the thesis is given below.

(i)  The second chapter deals with the review of the control of HVDC link covering basic modes of operation of a converter, different types of grid control systems and firing methods.

(ii) The third chapter is devoted to the problem (i) mentioned above.  The method of simulation and the results are reported.

(iii) The review of stability of parallel AC/DC systems is attempted in fourth chapter.

(iv)  A two machine system is simulated and the results showing the influence of the HVDC link controls on the connected AC system are given in the fifth chapter.

# CHAPTER 2

## CONTROL OF HVDC LINK

### 2.1 INTRODUCTION

The basic control system of a HVDC link controls the direct current at the rectifier end and extinction angle in the inverter. When it is desired to control the other quantities such as transmitted power or frequency of the AC network, a higher level control system generates the required current order. This chapter deals with the basic modes of operation of a converter and the details of the HVDC link control.

### 2.2 NORMAL MODES OF OPERATION OF A CONVERTER

For the normal modes of operation, the combined current-voltage characteristics of rectifier and inverter are shown in Fig.2.1.

From the converter theory the voltage equations are given by

$$V_{dr} = \frac{3\sqrt{2}}{\pi} E_{sr} \cos \alpha - \frac{3X_{cr}}{\pi} I_{dc}$$

and

$$V_{di} = \frac{3\sqrt{2}}{\pi} E_{si} \cos \gamma - \frac{3}{\pi} X_{ci} I_{dc}$$

where $V_{dr}$ -  DC voltage at the rectifier end

$\quad\quad V_{di}$ -  DC voltage at the inverter end
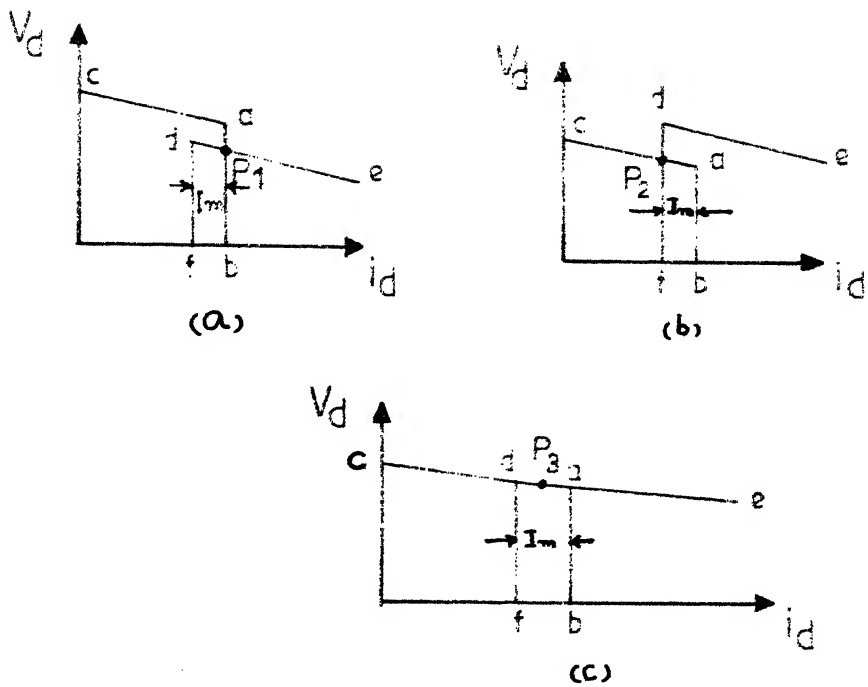
$\quad\quad I_{dc}$ -  DC current

FIG.2.1 CURRENT VOLTAGE CHARACTERISTICS
OF CONTROL SCHEME

$\alpha$ - Firing angle of the rectifier

$\gamma$ - Extinction angle of the inverter

$E_{sr}$ - RMS value of the commutating bus voltage at the rectifier end

$E_{si}$ - RMS value of the commutating bus voltage at the inverter end

$X_{cr}$ - Line commutating reactance for rectifier

$X_{ci}$ - Line commutating reactance for inverter.

The constant current control portion of the rectifier characteristic is portrayed by the line section a-b and the constant minimum alpha portion is shown as line segment a-c. The constant extinction angle portion of the inverter characteristic is d-e and the constant current control portion is d-f.

In the primary mode of operation of the converters, the rectifier constant current characteristic a-b crosses the inverter extinction angle characteristic d-e at operating point P1 as shown in Fig. 2.1(a). Under these conditions the rectifier controls the DC link current and inverter controls the voltage. This is to keep the reactive power low and to keep the voltages at rectifier and inverter as high as possible.

When the AC voltage at rectifier end is too low with respect to the AC voltage at the inverter end the situation is as shown in Fig.2.1(b). Then the inverter

current characteristic d-f crosses the rectifier constant α characteristic a-c at point P2 and current is maintained at current order minus $I_m$, the current margin which is defined as the amount by which the transmitted current decreases when the inverter current control loop is forced into action by AC system voltage conditions.

In the steady state, the inverter transformer load tap changer is controlled automatically to optimize the DC voltage and the rectifier load tap changer is controlled to hold the firing angle at some nominal value such as 12 - 18 degrees. During transient conditions both DC line voltage and rectifier angle may depart from the steady state values but the direct current is maintained at either the current order or the current order minus $I_m$ as the case may be.

A third mode occasionally occurs where the rectifier is operating on its minimum α characteristic and the inverter on its constant γ characteristic as shown in Fig.2.1(c). The direct current lies between current order and current order minus $I_m$ and is determined by the AC system voltages and the rectifier and inverter characteristics. This is a transition mode seen occasionally during AC system voltage swings resulting from faults and switching in the AC systems.

As seen from the above discussion the important characteristics of converter are (i) constant current control (ii) constant minimum ignition angle control and (iii) constant extinction angle control, the details of which are given below.

(i) Constant current control:  If the measured current in a rectifier is less than the set current, the firing angle of the rectifier α must be decreased in order to  increase cos α and thus raise the internal voltage of the rectifier.The difference between the internal voltages of the rectifier and inverter is thereby increased, and the direct current is increased proportionally.  If the measured current exceeds the set current, α must be increased instead of decreased, and all the quantities above are changed in the opposite sense.  This is the case when the constant current control is at the rectifier end.

If the constant current control is at the inverter end and if the measured current is too low, the internal voltage must be decreased by decreasing the α for the inverter. When the current is high, α for the inverter has to be increased.

(ii) Constant minimum ignition angle control: Converters exhibit a natural rectifier ceiling limit at α = 0° corresponding to each valve conducting almost immediately when its anode becomes positive with respect to cathode.  For a converter, in which each valve is a single unit, this is a possible mode of operation, though slight irregularity in the instant of firing may occur.  For valves consisting of each of several parallel-connected units with thyristors or multianode mercury arc valves, it is preferable to avoid firing of any valve until its anode voltage is appreciably

positive, to avoid the risk of any valve misfiring and consequently giving overcurrents in others. Thus, the lower value of α can be chosen as 5°.

(iii) Constant minimum extinction angle control: For operation at full inversion it is usually desirable to operate with α as nearly to 180° as possible in order to reduce the reactive power in the AC system. The practical limit is usually α = 140° - 170° such that extinction angle γ is adequate for valve deionization plus a margin to prevent commutation failures for minor AC system transients. The margin angle γ is defined as the time (in electrical degrees) from current reaching zero in a particular valve, to the time its anode voltage next crosses zero. Minimum values normally used for γ lie between 15° to 20°.

## 2.3 DETAILS OF CONTROL SYSTEM

The block diagram of a HVDC control system is shown in Fig.2.2. The major blocks of the control system are (i) Power controller (ii) Auxiliary controller (iii) Current controller (iv) Firing angle control and (v) Gama controller.

Power controller: A common requirement of a DC line is to deliver a scheduled value of power. If the DC voltage remains constant, by using the constant-current control we can achieve the said requirement. However, more accurate power control can be obtained automatically varying the direct current so as to compensate for changes in direct
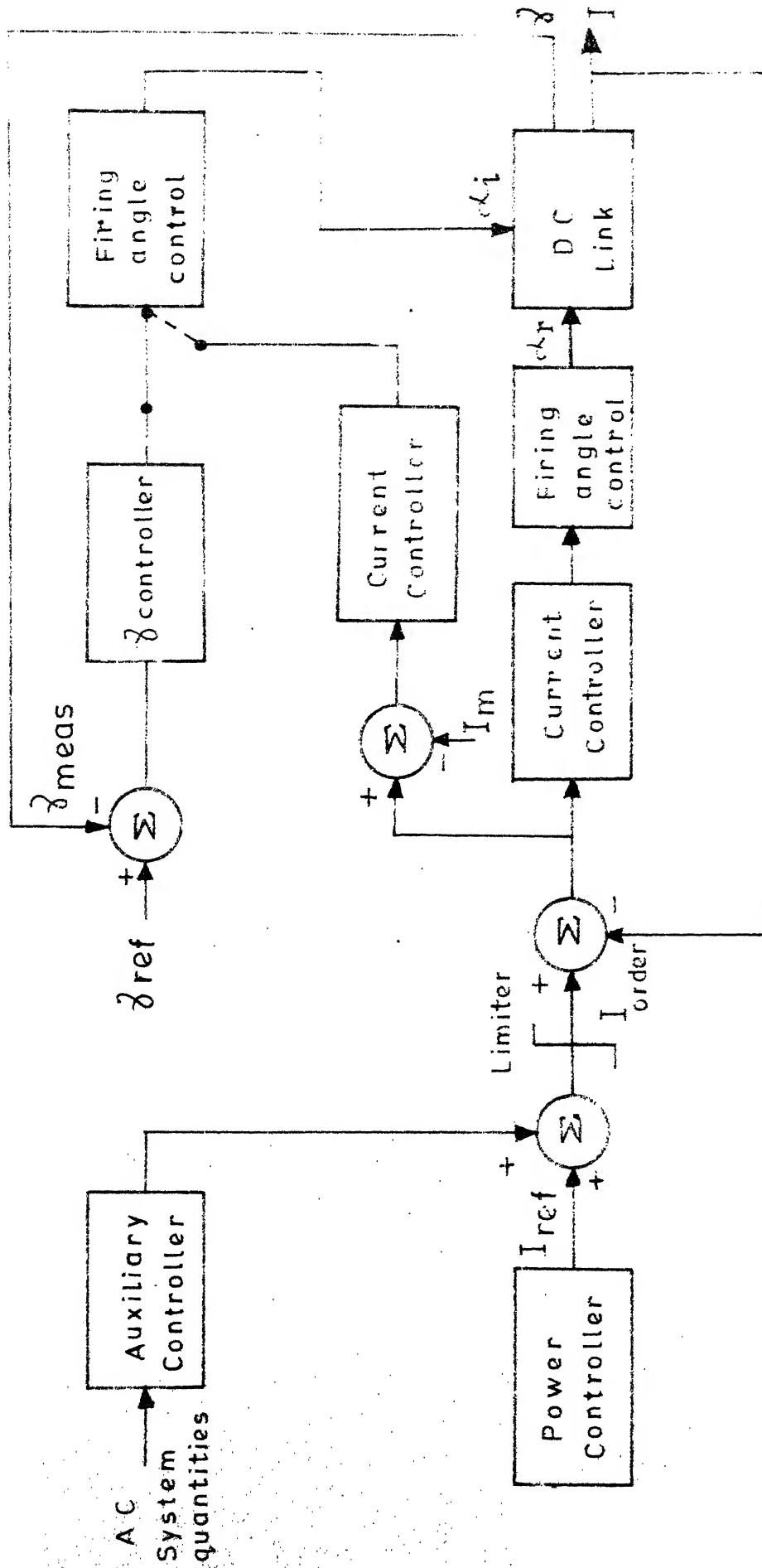
FIG.2.2 HVDC CONTROL SYSTEM

voltages caused by variation of line resistance, variation
of alternating voltage beyond that which can be corrected
by tap changers of grid control and by outages of one or more
valve groups.

Thus the current order $I_{ref}$ is output of the power
controller obtained by the division of power $P_{ref}$ by $V_d$,
the DC system voltage.

Auxiliary controller: The objective of this control
system is to introduce an external control signal.
This signal can be derived from the AC system to which the
DC link is connected. The purpose of the external control
signal is to stabilize the AC system by modulating the power
in the DC link . The signals that can be chosen from the AC
system are frequency, machine angle difference, power or
combination of some of these signals.

Limits on I order: The purpose of the maximum current
limit is to avoid thermal damage to the valves and that of
minimum current limit is to avoid operation with discontinuous
current which leads to overvoltages.

Current controller: It consists of an amplifier and a
phase shift circuit. The error signal which is the difference
of the actual DC line current $I_{dc}$ and the reference value
$I_{ref}$ is the input to the controller and the output is a
control voltage that determines the firing angle of the
converter.

Gama controller:   It is required for control of extinction angle in the inverter  There are two methods which have been used for this.

(i) Measurement of $\gamma$ and steps to improve it in the next cycle which is a feedback type control and is as shown in the block diagram.

(ii) Continuous precalculation of $\gamma$ on the basis of the facts already known before the firing instant, and initiation of firing impulse at the proper instant.  This is an open loop control, also known as predictive type of control system.

The predictive type of control systems are fast in action but not quite accurate.  On the other hand, the feedback type of control systems involve the measurement of $\gamma$ and thus are slow but fairly accurate.

Firing angle control:  There are two methods of firing, (i) Individual phase control and (ii) Equidistant pulse control.  Both the methods can be employed for controlling firing pulses for the rectifier and the inverter valves.

(i) Individual phase control:   This method depends directly on the AC system voltage.  The characteristic of the grid control is the determination of the control angle for each valve from the voltage zero point of the corresponding commutation voltage on the secondary side of the converter transformer.  As shown in Fig.2.3 a saw tooth voltage is triggered at the voltage  zero of a commutation voltage
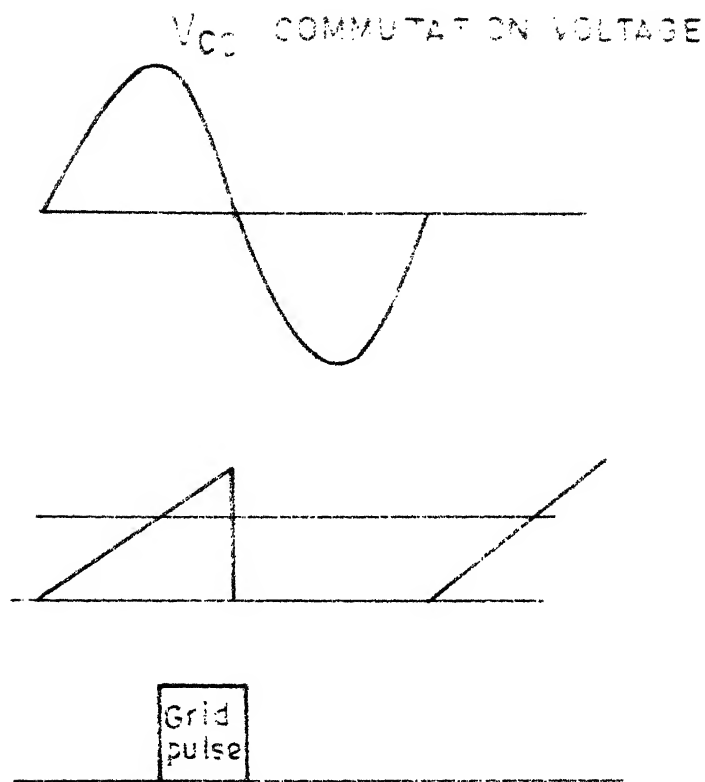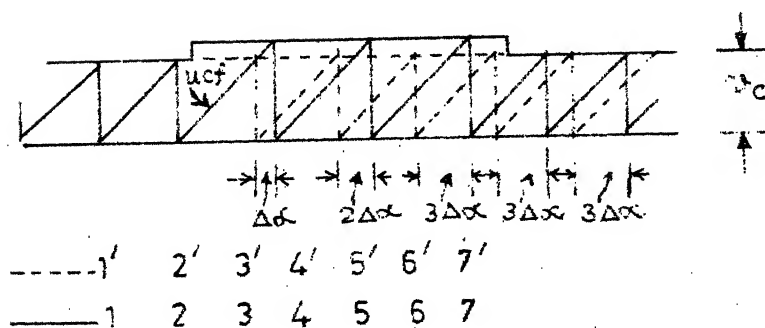
FIG.2.3  INDIVIDUAL PHASE CONTROL



-----UNCHANGED VOLTAGE WITH IMPULSE SEQUENCE 1'2'---
——— VOLTAGE  CAUSING INCREASE OF FIRING ANGLES
    WITH  IMPULSE  SEQUENCE 1,2---

FIG.2.4  EQUIDISTANT  FIRING ANGLE CONTROL

and compared with a control voltage $VC_1$. When the saw tooth
voltage crosses the value of the control voltage $VC_1$, a
firing pulse of width 120° is given. The control voltage
$VC_1$ can be given from a current controller or extinction
angle controller.

A drawback of the individual phase control is the
tendency to generate non-characteristic harmonics resulting
in harmonic instability particularly with high impedance
AC networks. This is caused by the voltage feedback which
is established by deriving the control function directly
from the filter bus voltage.

(ii) Equidistant pulse control: This method was first
suggested by Ainsworth [ 7 ] to obtain equally spaced pulses
using a phase-locked oscillator.

In this method the control function $u_{cf}$ which can
be derived from the commutation voltage has a constant slope
as shown in Fig.2.4, and initiates the control impulse at
the intersection with the voltage $u_c$ generated by the
controller. At the same time it returns to its initial value
and then begins to rise again. The distance between the
consecutive pulses is therefore equally long and is determined
by the magnitude of $u_c$ and by the slope of the control function
$u_{cf}$. The train of pulses is resolved by a ring counter dis-
tributing them to the individual valves.

In the equidistant pulse control systems the
synchronization of oscillator takes place with the help of

main current control loop or extinction angle control loop.
A change in the control voltage changes directly the fre-
quency of the oscillator. Therefore these grid control
systems are also known as pulse frequency control systems(PFC)
and have the following drawbacks:

(i) These control systems have an integral characteris-
tic in the grid control unit. So it is not possible without
special devices to operate the converters with constant
control angle   .

(ii) The linearization of the converter control
characteristic, the ratio of output voltage of the converter
$V_d$ and of the input voltage of the grid control system $VC_1$
is not possible with simple means.

To overcome these drawbacks a new grid control
system called the pulse phase control system (PPC) was
proposed by Rumpf and Ranade [6] in which the change in
the control voltage $VC_1$ causes a proportional change in the
control angle $\alpha$.

# CHAPTER 3

## SIMULATION OF HVDC TRANSMISSION SYSTEM
## AND ITS CONTROLS

### 3.1 INTRODUCTION

This chapter deals with the mathematical modelling
and simulation of HVDC transmission system and its controls
on a Digital computer. The DC link considered is a short
link or a back to back link.

### 3.2 FORMULATION

The study of DC link is based on the system shown
in Fig.3.1 in which the AC system voltages are represented
as constant voltage sources.

The formulation is based on the following
assumptions:

(i)     Harmonics in DC current are ignored.

(ii)    Nonlinearities such as the saturation of
        transformers are neglected.

(iii)   There is no time delay in the measurement of $\gamma$
        and the current.

Fig.3.2 shows the block diagram of the power
controller which has been explained in the last chapter.
This is a higher level control system to control the DC
link current and also to effect the connected AC system
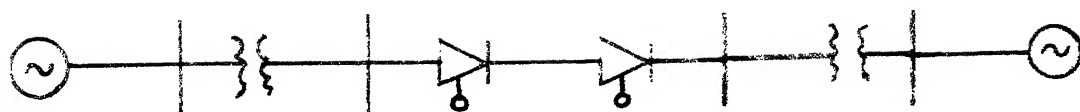stability by virtue of the external control signal. This
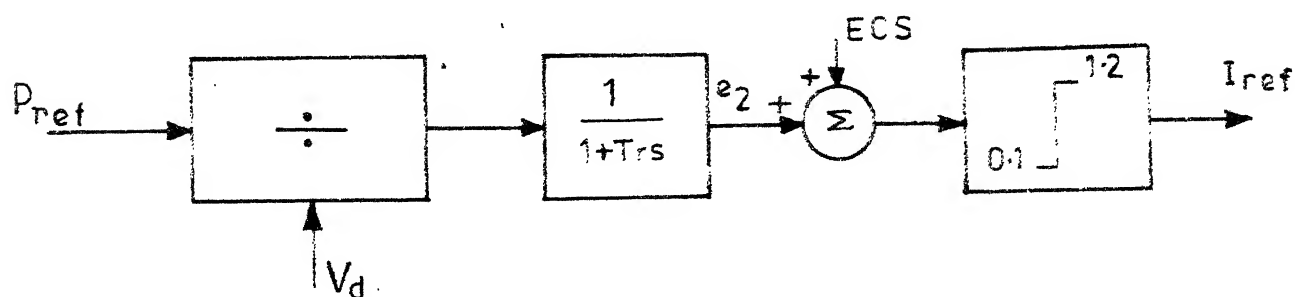
FIG.3.1  SYSTEM  DIAGRAM
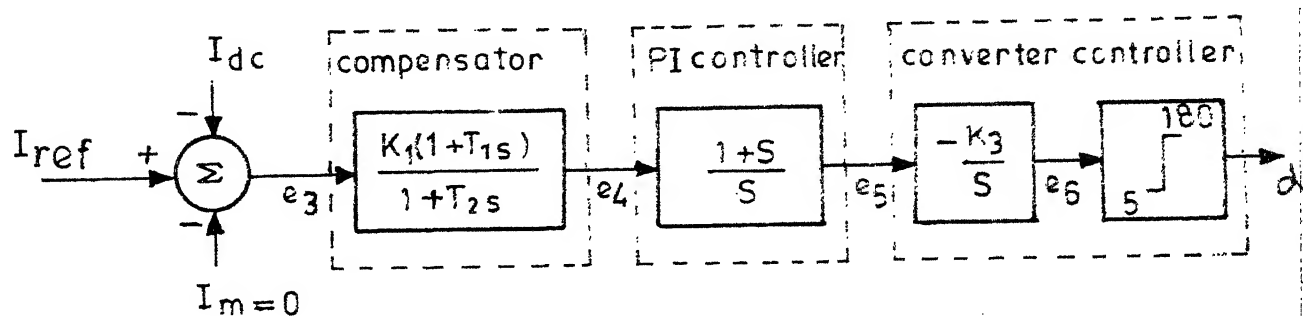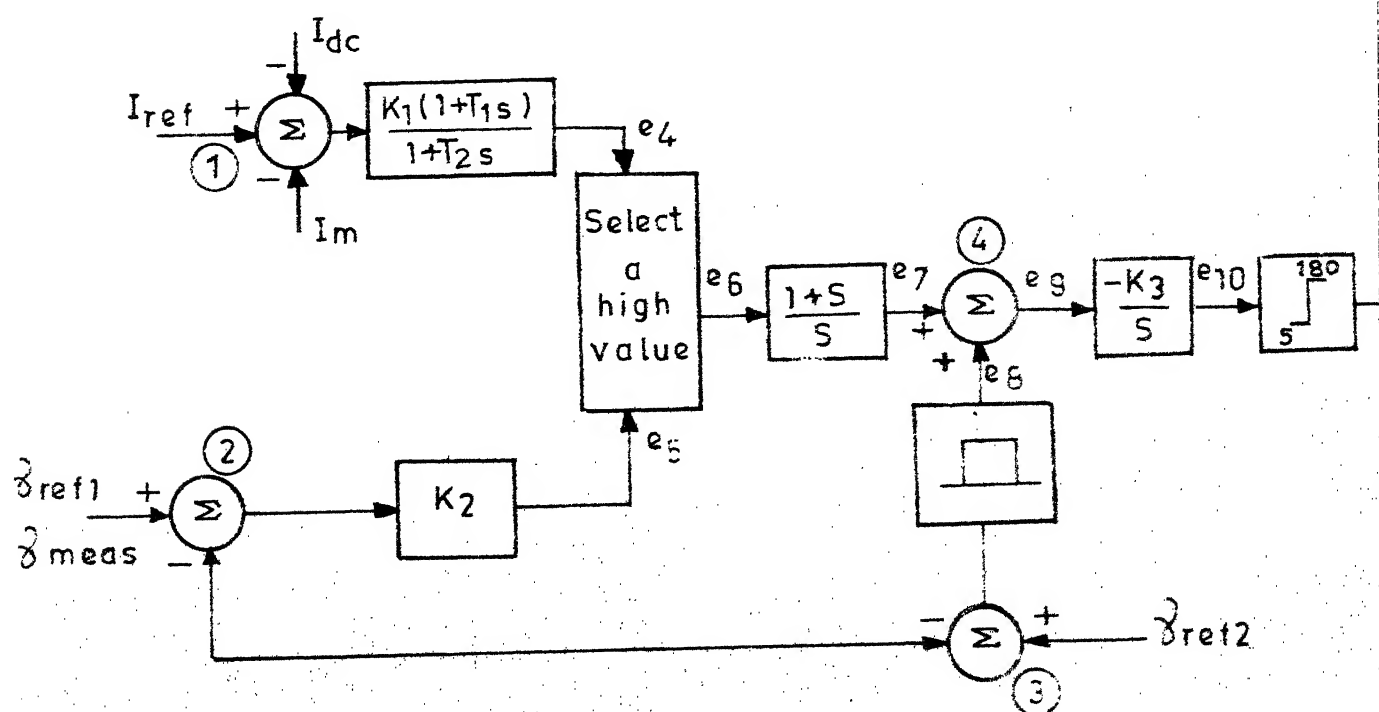


FIG.3.2  POWER CONTROLLER



FIG.3.3  RECTIFIER CONTROL

control signal is derived from the AC system quantities that
vary during the system disturbance. The current or power level
of parallel AC lines, the total flow between the buses or the
frequency and rate of change of frequency at a given bus could
conceivably be used to generate a useful control signal.

However, as the simulation is restricted to HVDC
system alone, this ECS has not been taken into account.

Figs. 3.3 and 3.4 show the block diagrams for closed
loop control of $\alpha_r$ for the rectifier and $\alpha_i$ for the inverter
respectively.

Inverter control loop: The current measured from the
DC link $I_{dc}$ is fed to the summing junction 1 along with the
signal $I_{ref}$, the current order and $I_m$, the current margin.
Gama measured is fed to the two summing junctions 2 and 3.
Whenever Gama is less than GAMEREF2 a single pulse is
generated and fed to the junction 4. The purpose of the
single pulse is to make the Gama control faster and to avoid
the commutation failure. $e_5$ is compared with $e_4$. $e_6$ will be
the highest of these two. This comparison results in a
smooth transition from constant extinction angle control
mode to the constant current control mode and vice-versa.
The significance of $\alpha$ limits has been explained in the
last chapter.

## 3.3 SYSTEM EQUATIONS

The following equations can be easily derived from the block diagrams of power controller, rectifier and inverter control loops.

From Fig.3.1,

$$\dot{e}_2 = \frac{1}{T_r}(\frac{P_{ref}}{V_d} - e_2) \tag{3.1}$$

From Fig.3.2, the block diagram of rectifier control loop the following equations can be obtained:

$$\dot{e}_4 = \frac{1}{T_2}(K_1(I_{ref}-I_{dc}) + K_1 T_1 \frac{d}{dt}(I_{ref}-I_{dc})-e_4) \tag{3.2}$$

$$\dot{e}_5 = e_4 + \dot{e}_4 \tag{3.3}$$

$$\dot{e}_6 = -e_5 K_3 \tag{3.4}$$

From Fig.3.3, the block diagram of inverter control loop the following equations can be derived:

$$\dot{e}_4 = \frac{1}{T_2}((I_{ref}-I_{dc}-I_m)K_1+K_1 T_1 \frac{d}{dt}(I_{ref}-I_{dc}-I_m)-e_4) \tag{3.5}$$

$$e_5 = (\gamma_{ref1} - \gamma_{meas})K_2 \tag{3.6}$$

$$e_6 = Max(e_4, e_5) \tag{3.7}$$

$$\dot{e}_7 = e_6 \tag{3.8}$$

$$e_{11} = e_7 + e_6 \tag{3.9}$$

$$\dot{e}_{10} = -K_3(e_{11} + e_8) \tag{3.10}$$

From the converter theory,

$$V_{dr} = \frac{3\sqrt{2}}{\pi} E_r K_{2r} \cos \alpha - \frac{3}{\pi} K_{1r} K_{2r} X_{cr} I_{dc} \tag{3.11}$$

$$V_{di} = \frac{3\sqrt{2}}{\pi} E_i K_{2i} \cos \gamma - \frac{3}{\pi} K_{1i} K_{2i} X_{ci} I_{dc} \tag{3.12}$$

$$V_{di} = \frac{3\sqrt{2}}{\pi} E_i K_{2i} \cos \beta + \frac{3}{\pi} K_{1i} K_{2i} X_{ci} \tag{3.13}$$

Equation (3.11) can be used to determine the DC voltage at the rectifier end $V_{dr}$, the other quantities like $E_r$, $I_{dc}$, $X_{cr}$ being known. Equation (3.12) cannot be readily used to find out $V_{di}$ because $\gamma$ cannot be calculated without knowing the value of $V_{di}$. Thus equation (3.13) can be used in which $\beta = 180° - \alpha_i$, $\alpha_i$ being known, $V_{di}$ can be calculated and then using equation (3.12) the value of $\gamma$ can be calculated.

The purpose of the introduction of constants $K_{1r}$, $K_{2r}$, $K_{1i}$, $K_{2i}$ is to permit a flexible system of per unit values for DC variables and the equations are transformed such as to permit the use of per unit AC variables, defined independently. These constants are as defined in [8] are given below.

$$K_{1r} = \frac{1}{\sqrt{3}} \frac{I_{db}}{I_{br}} \tag{3.14}$$

$$K_{2r} = \frac{V_{br}}{V_{db}} \tag{3.15}$$

$$K_{1i} = \frac{1}{\sqrt{3}} \frac{I_{db}}{I_{bi}} \tag{3.16}$$

$$K_{2i} = \frac{V_{bi}}{V_{db}} \qquad (3.17)$$

where $I_{br}$ and $I_{bi}$ are the base values of AC currents at the secondaries of rectifier and inverter transformers, $V_{br}$ and $V_{bi}$ are the base values of AC voltages at corresponding terminals. The ratio of $K_{1r}/K_{2r}$ thus represents the ratio of base power of DC to AC. The advantage of this system is that common AC base quantities are independent of the DC base quantities.

The current in the DC link can be calculated by the equation

$$L\frac{di}{dt} = V_{dr} - V_{di} - I_{dc} R_{dc} \qquad (3.18)$$

where $V_{dr}$ and $V_{di}$ are defined by the equations (3.11) and (3.13).

The power at the rectifier end $P_r$ and $P_i$ the power at the inverter end are given by equations

$$P_i = V_{di} I_{dc} \qquad (3.19)$$

$$P_r = V_{dr} I_{dc} \qquad (3.20)$$

where $I_{dc}$ is the DC link current and $V_{di}$ and $V_{dr}$ being defined by the equations (3.11) and (3.13).

Finally $V_d$, the DC system voltage used in the power controller is chosen as the average of DC voltages at rectifier end and inverter end. Thus

$$V_d = \frac{V_{dr} + V_{di}}{2} \qquad (3.21)$$

3.4 DIGITAL SIMULATION:

(i) System data:

Parameters for the power controller:

Time constant $T_r = 0.35$

Parameters for the rectifier control loop:

Gains $\qquad K_1 = 7.2 \quad K_3 = 2160.0$

Time constants $T_1 = 0.01 \quad T_2 = 0.0033$

Parameters for inverter control loop:

Gains $\qquad K_1 = 7.2 \quad K_2 = 0.15 \qquad K_3 = 2160.0$

Time constants $T_1 = 0.01 \quad T_2 = 0.0033$

Gama ref1 $\qquad = 16°$

Gama ref2 $\qquad = 10°$

Current margin $I_m = 0.1$

Width of pulse $\qquad = 0.002$

Height of pulse $\qquad = 1.00$

Current limits:

Lower limit $\qquad = 0.1$

Upper limit $\qquad = 1.2$

Limits on $\alpha$ for both rectifier and inverter:

Lower limit $\qquad = 5°$

Upper limit $\qquad = 180°$.

DC line data:

Line resistance $R_{dc}$ = 0.02 p.u.

Line inductance = 0.01 p.u.

Line commutating reactance for rectifier $X_{cr}$ = 0.08 p.u.

Line commutating reactance for inverter $X_{ci}$ = 0.08 p.u.

Constants for conversion into p.u. quantities:

$K_{1r}$ = $K_{1i}$ = 1.38

$K_{2r}$ = $K_{2i}$ = 0.8625

(ii) Initial conditions:

Scheduled power $P_{ref}$ = 1.0

Scheduled voltage $V_d$ = 1.0

$\alpha$ for the rectifier = 12°

$\gamma$ for the inverter = 16°

(iii) Simulation:

The following cases are simulated by solving the system differential equations using a fourth order Runge-Kutta subroutine.

(a) $P_{ref}$ is changed to 0.8:

The aim of this study is to study the response of the DC system when the power order is decreased.

(b) $E_r$ is changed to 0.8.

(c) $E_i$ is changed to 0.85.

The purpose of both the above studies is to examine the response of the DC link controls when the AC system voltages at rectifier and inverter are reduced because of disturbances in the AC system.

The following graphs are plotted in each case.

(i)     DC current $I_{dc}$ vs. time.

(ii)    Firing angle $\alpha$ vs. time.

(iii)   Extinction angle $\gamma$ vs. time.

(iv)    DC voltage $V_{dr}$ vs. time.

(v)     DC voltage $V_{di}$ vs. time.

(vi)    DC power at rectifier end $P_r$ vs. time.

(vii)   DC power at inverter end $P_i$ vs. time.

## 3.5 DISCUSSION

(i) $P_{ref}$ changed to 0.8:

When $P_{ref}$ is changed to 0.8 the DC system response
is shown in Figures.3.5 and 3.6. Since the power order is
decreased and the voltages are slightly more than 1.0 in
steady state the steady state value of the current $I_{dc}$ is
less than 0.8. The value of $\alpha$ is increased to 13°. Because
of the integral characteristic the $\gamma$ value remains constant
at 16°. The response is fast, the current $I_{dc}$ and the powers
$P_r$ and $P_i$ reaching the steady state     in 2.0 seconds
with no oscillations. The firing angle $\alpha$ and the extinction
angle $\dot{\gamma}$  settle to steady state values in 0.8 seconds.

(ii) $E_r$ changed to 0.8:

In this case, it can be observed from Figs.3.7
and 3.8 that the value of $I_{dc}$ first falls to 0.9 p.u. but
subsequently raised to 1.1 p.u. in 0.8 seconds. The firing

angle $\alpha$ decreases to maintain the current but is limited
by the lower limit on $\alpha$ to 5°. Hence the current control
has been transferred to the inverter end. The value of $\gamma$
is increased to 36.3° so that the value of $V_{di}$ becomes less
and thus the DC current can be maintained at a value which is the
reference minus margin. The response is good with no
oscillation with the DC current and powers at rectifier and
inverters reaching steady state in 0.8 seconds. $\gamma$ settles
to its new value is about 0.2 seconds with little overshoot.

(iii) $E_i$ changed to 0.8:

As shown in Figs.3.9 and 3.10, the value of DC
current after a few transients increases and reaches a value
of 1.166. The constant current control is at rectifier end.
The value of $\alpha$ is increased to take care of the decrease in
the AC voltage at inverter end. The final value of $\gamma$ is
16°. DC voltages at both rectifier and inverter
are decreased because of the decrease in AC voltage at inverter
end. The powers $P_r$, $P_i$ finally reach the steady state values
which are nearly equal to the prefault powers respectively.
The steady state values are reached in about 2.0 seconds. The
time taken for $\alpha$ and $\gamma$ to settle in less than 0.2 seconds
which shows the effectiveness of the control.

3.6 CONCLUSION

The values of the system parameters are taken from a
practical system but no attempt has been made to optimize the
parameters. The response seems to be acceptable for the
control purposes.

FIG. 3.5

STEP CHANGE IN $P_{ref}$
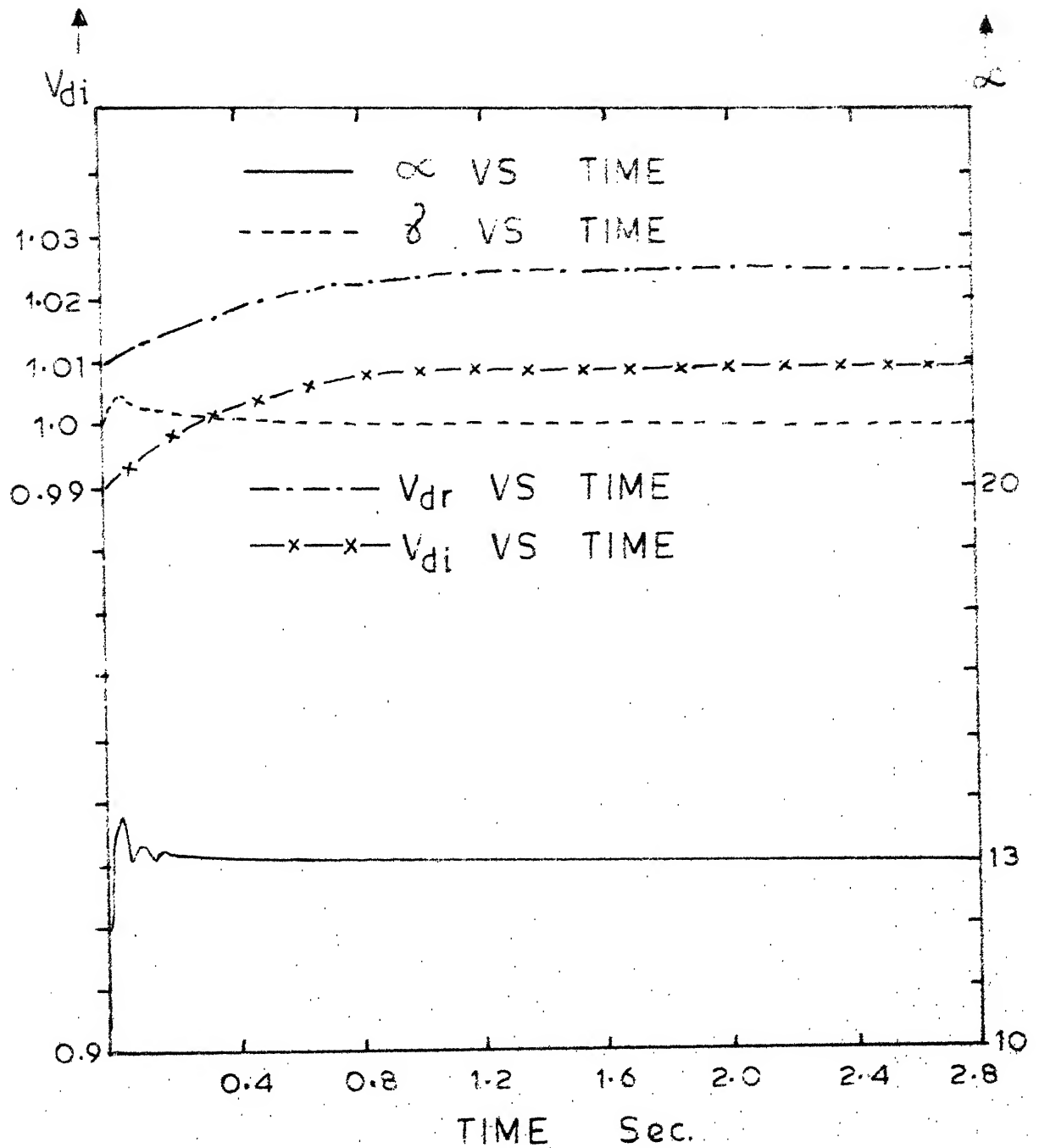
VARIATION OF $\propto$, $\delta$, $V_{dr}$, $V_{di}$ VS TIME
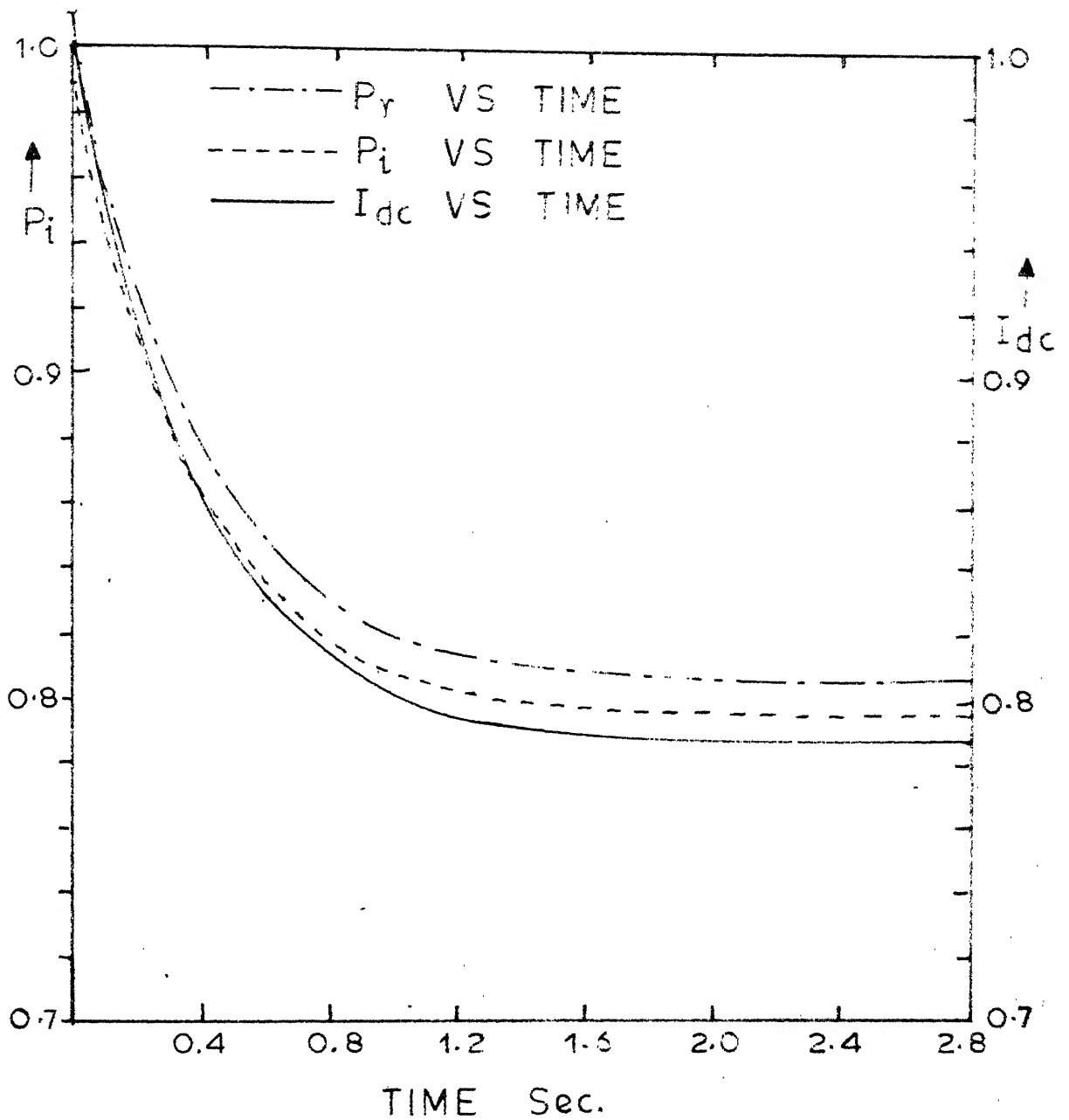
FIG. 3·6

STEP CHANGE IN $P_{ref}$

VARIATION OF $P_r$, $P_i$, $I_{dc}$ VS TIME
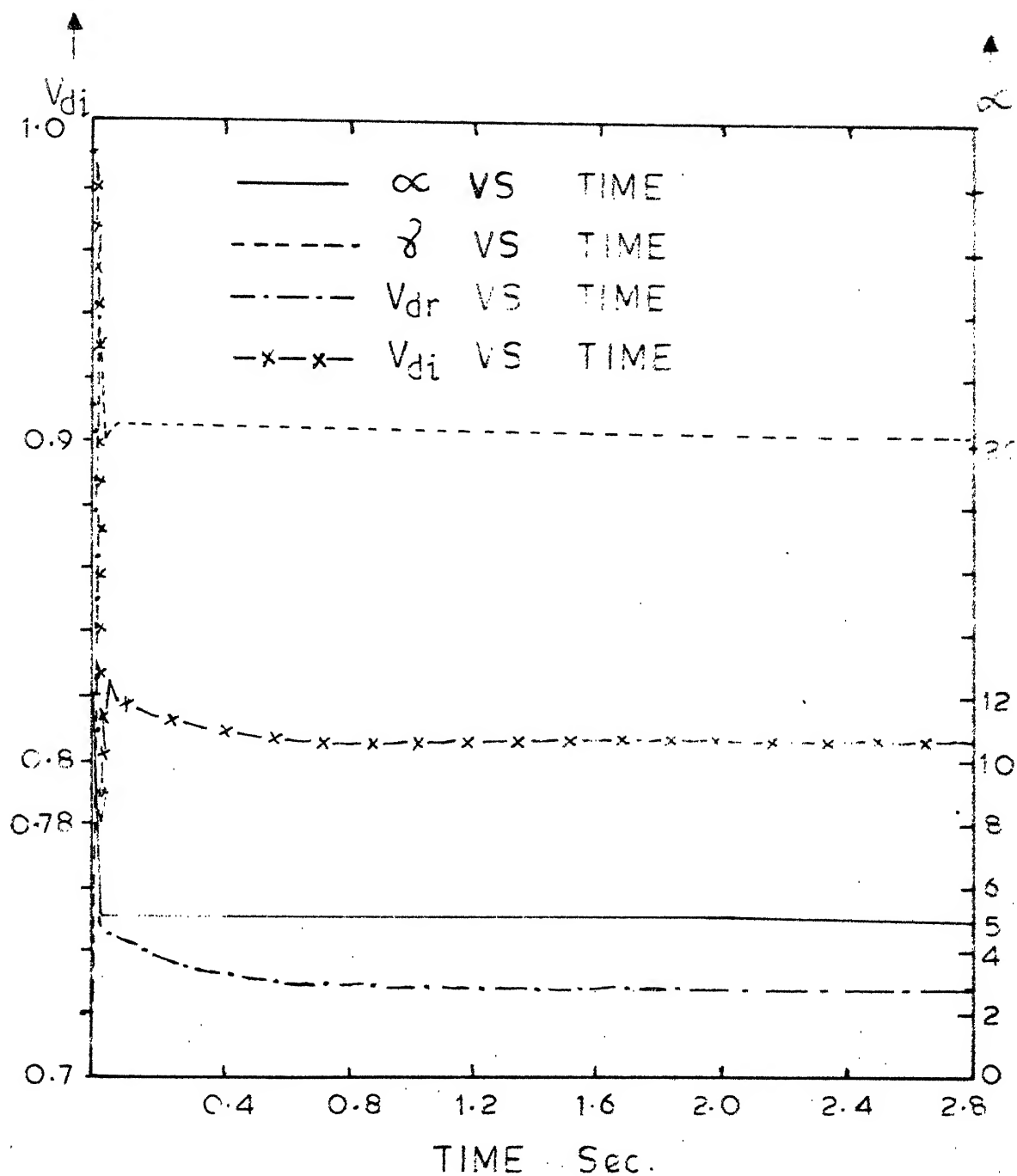
FIG. 3·7

STEP CHANGE IN RECTIFIER AC VOLTAGE
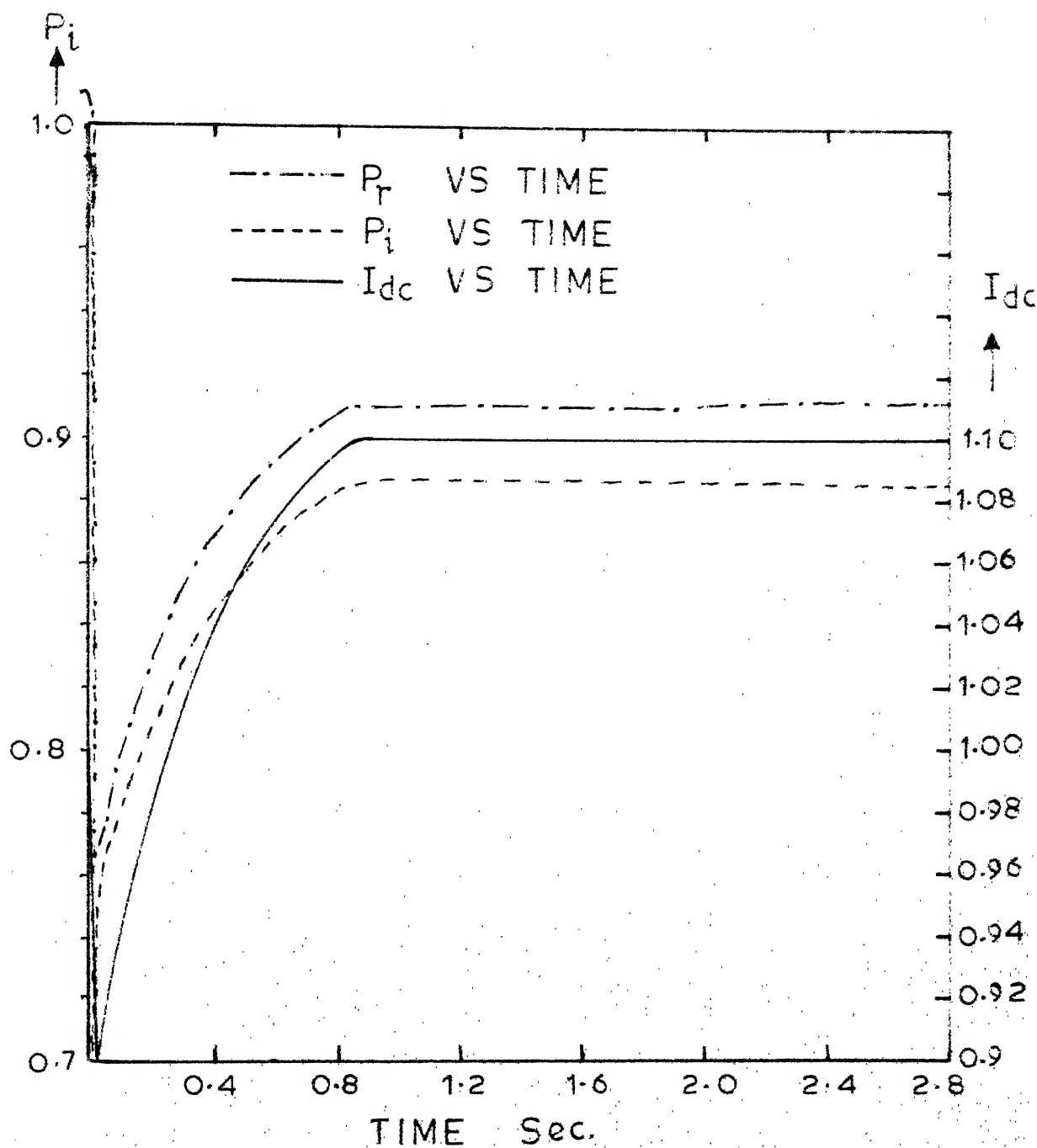VARIATION OF $\propto, \gamma, V_{dr}, V_{di}$ VS TIME

FIG.3·8

STEP CHANGE IN RECTIFIER AC VOLTAGE
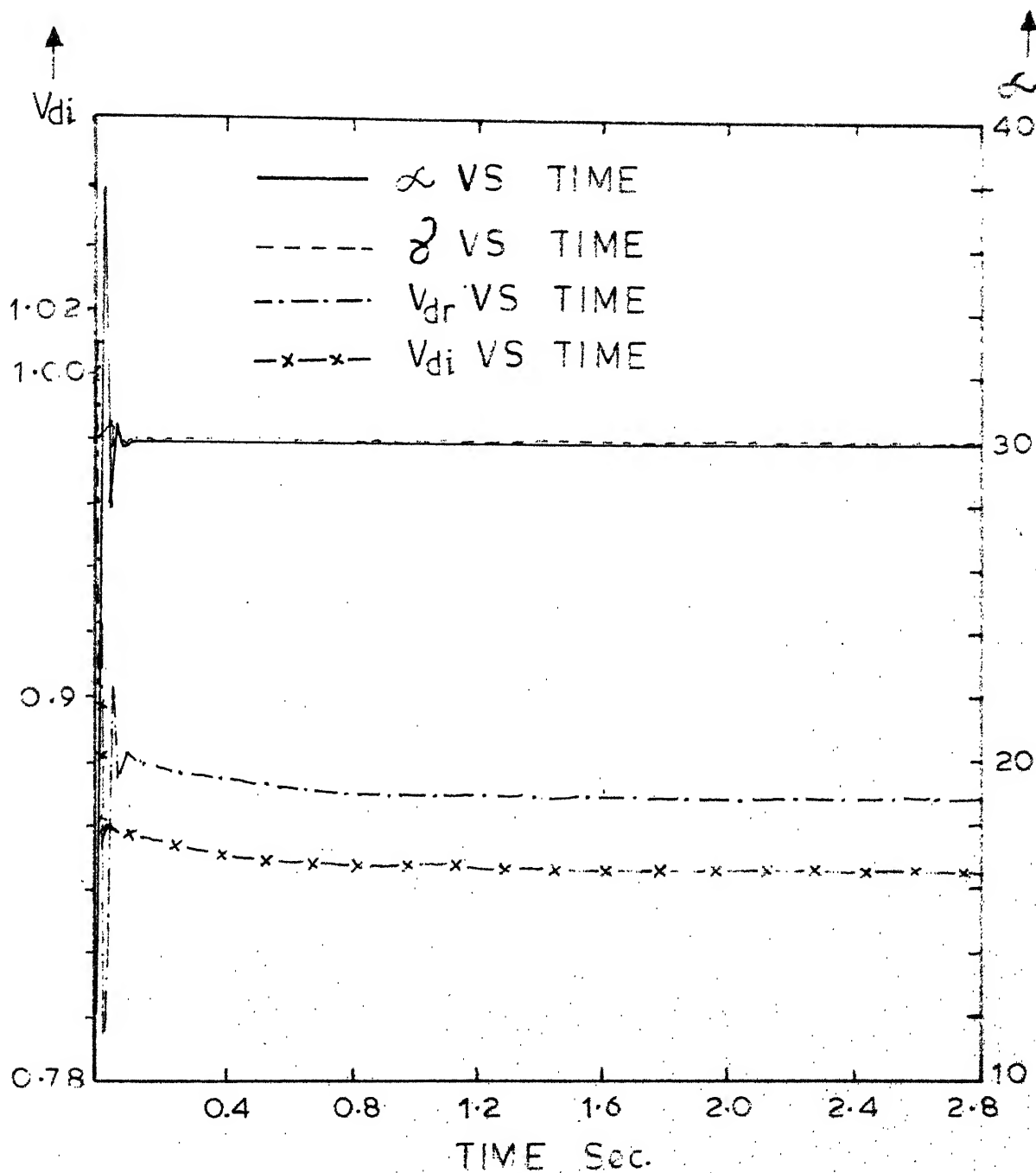VARIATION OF $P_r$, $P_i$, $I_{dc}$ VS TIME

FIG. 3·9

STEP CHANGE IN INVERTER AC VOLTAGE
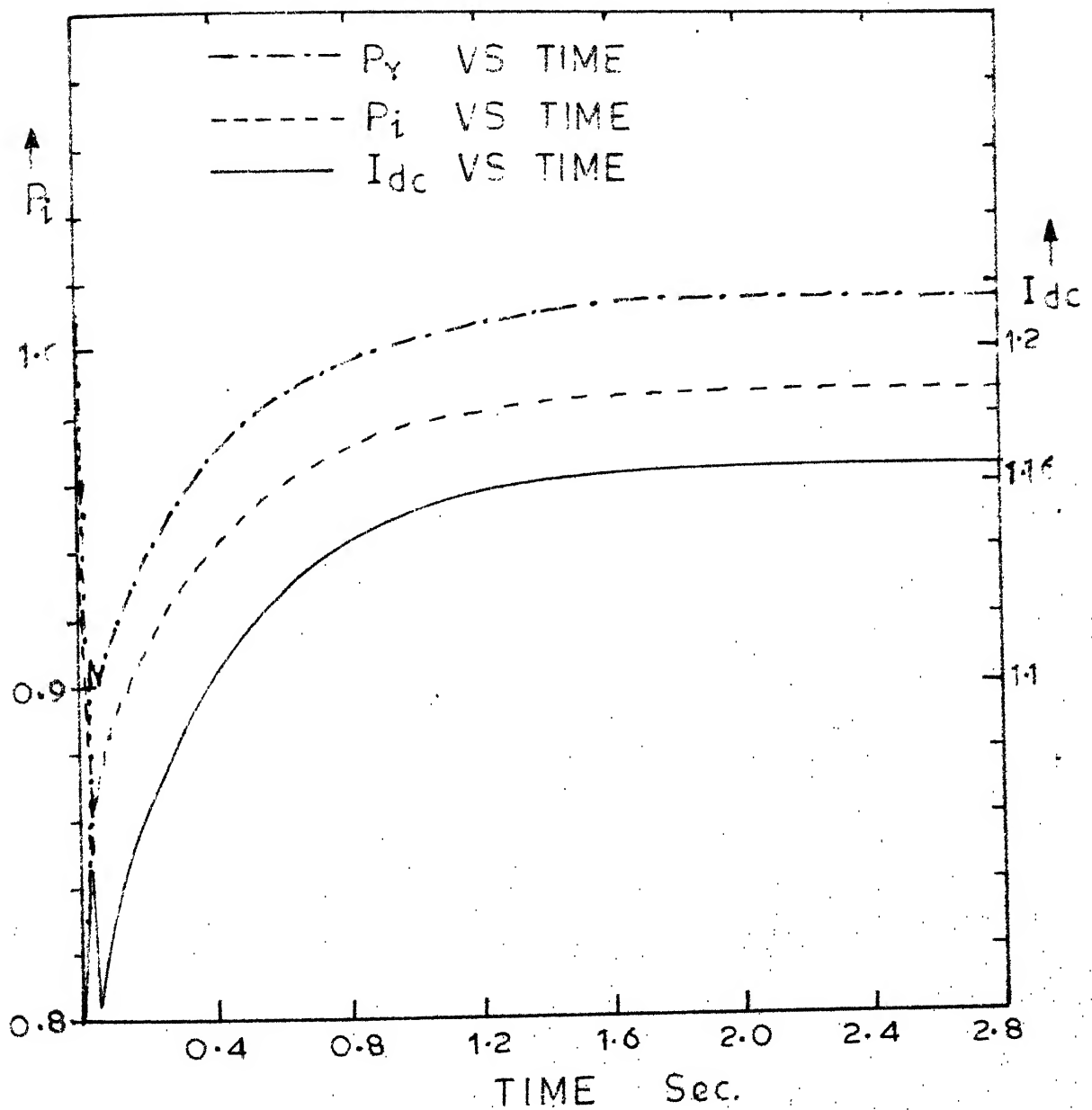VARIATION OF $\propto$, $\gamma$, $V_{dr}$ $V_{di}$ VS TIME

FIG. 3·10

STEP CHANGE IN INVERTER AC VOLTAGE
VARIATION OF $P_r$, $P_i$, $I_{dc}$ VS TIME

# CHAPTER 4

## STABILITY OF PARALLEL AC/DC SYSTEMS

### 4.1 INTRODUCTION

Whenever a disturbance occurs in a large AC system, temporary use is made of the mechanical energies stored in the different machines to meet the new system conditions which makes the frequency of each machine to vary. The integral of the frequency difference between the machines causes an exchange of power flow through the electrical network to lead the system to a new position of balance with the same frequency on all the machines in steady state. This is the condition when the system is considered to be stable. On the other hand, if the angles between the different machines increase monotonically, the system is considered to be transiently unstable. The transient stability of the AC system can be improved by additional means like series capacitors and generator excitation control. The inherent ability of the fast response of a DC system and the possibility of modulating the power flow through the DC link can be used to improve the stability of an AC system to which the DC link is connected. The effectiveness of HVDC system in increasing system damping has been demonstrated successfully in recent years in the EEL River HVDC back to back tie, Pacific Coast intertie and the recently commissioned Square Butte HVDC

In this chapter, a brief review of the literature on stability of parallel AC/DC systems is presented.

## 4.2 REVIEW

The idea of stabilization of an AC link by a parallel DC link was first given by Uhlmann [9]. By considering an idealized, two machine system with parallel AC/DC links, proportional and integral control using the frequency difference of the interconnected networks causes significant improvement in the system dynamic stability. It was also shown that a control signal proportional to the frequency difference increases the damping in the system, whereas the integral of the frequency difference has the effect of increasing the synchronizing torque coefficient.

The other papers which were subsequently published in this area are by Peterson, Machida, Kauferle, Dougherty and others [10-16], confirm the effect of DC link controls on system stability.

In another paper published by Uhlmann [17] the control effect of the DC link on the transient stability of a two-machine system was tested by using the digital simulation. In addition to the earlier results presented by him, it was shown that the damping introduced by the DC link control remains satisfactory even under practical current limitations on the DC link.

The extension of the Uhlmann's work was reported in [18] considering the effect of the dynamics of the power controller and the system reactances by a linearized eigen value analysis of a two machine system with parallel AC and DC links.

In the earlier papers, the generator was represented by the simple model of constant voltage behind transient reactance. In a recent paper [19] the dynamic stability of a two machine system using the dynamic characteristics of the electrical machines is presented.

The application of the theoretical concepts of stability improvement through DC link controls on actual systems was first reported for the EEL River back to back link. Both the design aspects of an external control system and its operational experience has been reported in [20] and [21]. Recently, the design and testing of the controller for Pacfic intertie has been reported [22,23] and it has been claimed that the steady state stability limit on the parallel AC link has been increased by the introduction of the controller which utilizes AC link power deviation as the input signal.

# CHAPTER 5

## DIGITAL SIMULATION OF A PARALLEL AC/DC SYSTEM

### 5.1 INTRODUCTION

By using fast acting controls on HVDC link, it is possible to improve the stability characteristics of an interconnected power system. The possibility of introducing more damping in AC system and thus improving the stability of the existing system through the addition of external control signals to rapidly modulate the power transmitted by a DC link has been reported in many of the recent publications [10-16].

This chapter deals with the simulation of a two machine system with parallel AC and DC links and investigation of the effect of the DC link controls on the improvement of stability.

### 5.2 SYSTEM MODEL

The two machine system considered is shown in Fig. 5.1. In the system considered, each machine can be considered to be an equivalent machine for an area when all the machines are swinging together. 1 and 2 are generator terminal buses where a local load at each bus is connected. $X_5$ and $X_6$ are the generator internal reactances. There are two AC lines and a DC line connected in parallel between the buses 3 and 4. $X_0$ is the reactance of each AC transmission line. $X_3$ is the reactance of the transmission line which is
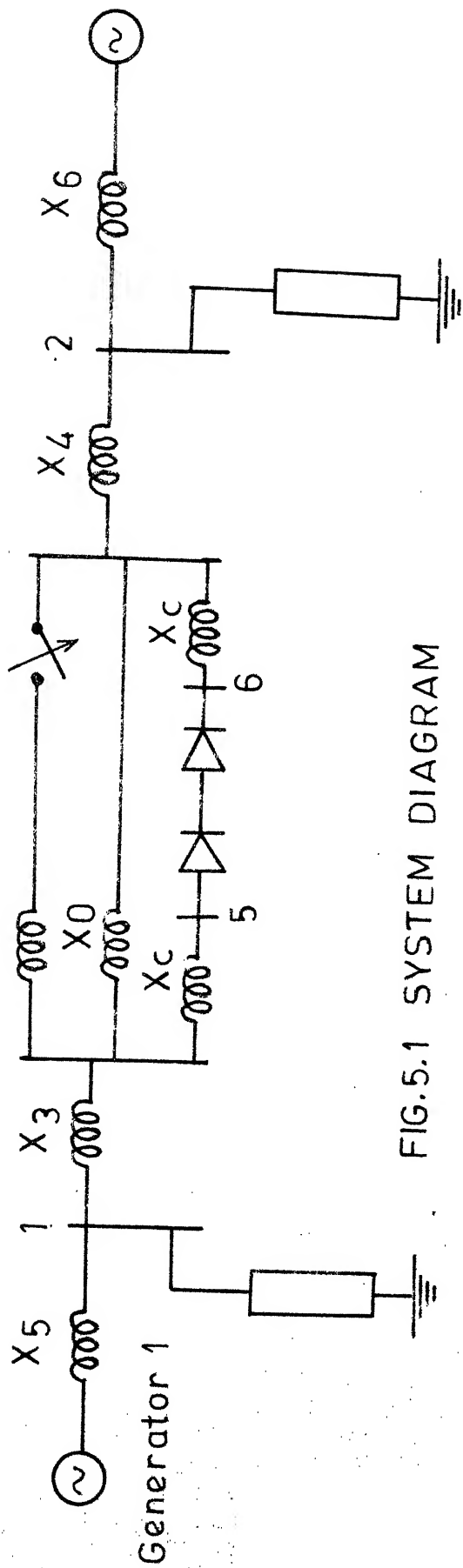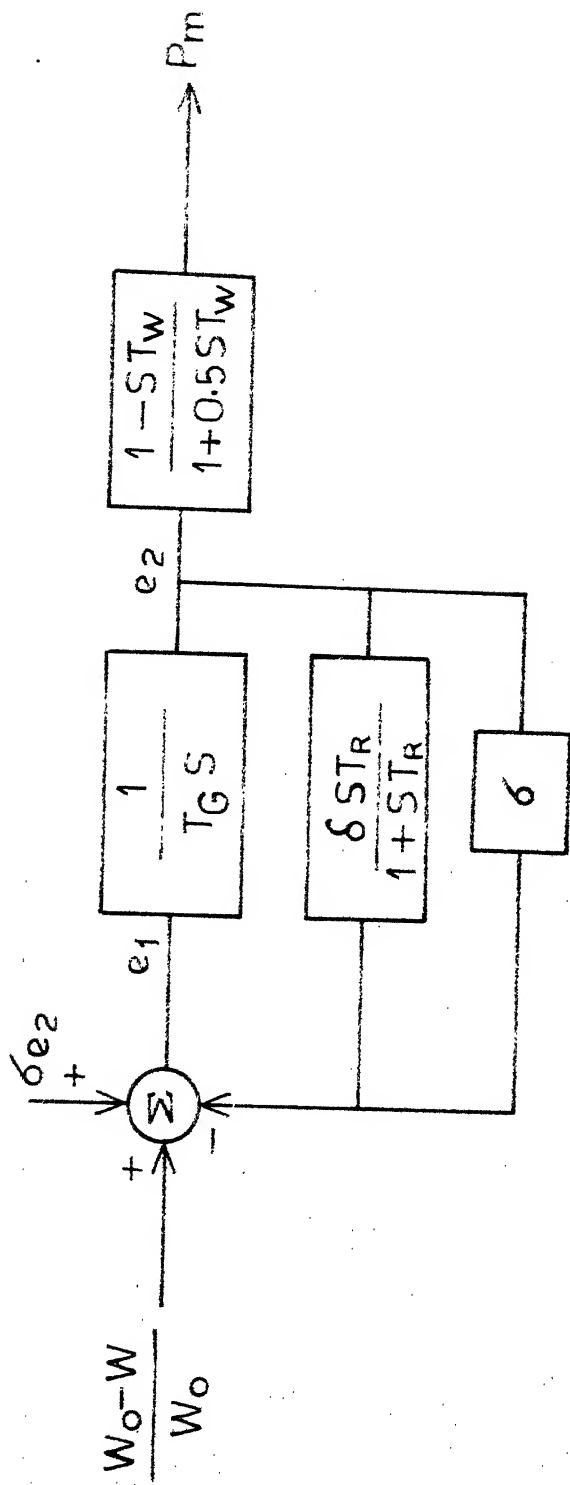
FIG.5.1 SYSTEM DIAGRAM



FIG.5.2 HYDRO-GOVERNOR-TURBINE SYSTEM

connected between buses 1 and 3. Similarly, $X_4$ is the reactance of the transmission line which connected between buses 2 and 4.

5.2.1 Basic Assumptions:

The formulation given below is based on the following assumptions:

(1)   The generators are represented by constant voltage sources behind transient reactances.

(2)   Exciter action is ignored.

(3)   Line resistance and capacitance are ignored.

(4)   The DC link is represented by a simplified model discussed in [8] where the dynamics in the power controller are considered but converter controller dynamics are ignored. Transients in the DC line are also ignored.

(5)   The harmonic components of the DC and AC currents introduced by the converter are ignored.

5.2.2 Generator Representation:

As the generators are represented by the classical model, only the electromechanical equations are considered which are

$$\frac{d\,\delta_i}{dt} = W_i - W_o \tag{5.1}$$

$$\frac{d\,W_i}{dt} = \frac{\pi f}{H_i}\,(Pm_i - Pe_i) \tag{5.2}$$

where $H_i$ = inertia constant,

$\delta_i$ = machine angle of ith machine,

$W_i$ = actual speed of the ith machine,

$W_o$ = synchronous speed,

$f$ = system nominal frequency

$Pm_i$ = mechanical power input to the ith machine,

$Pe_i$ = electrical power output of the ith machine.

The mechanical power input to the machine is obtained from the output of the hydro-governor-turbine system shown in Fig.5.2. The equations for the governor-turbine system are

$$e_1 = \frac{W_o - W}{W_o} - e_3 - \sigma e_2 + \sigma p_m \qquad (5.3)$$

$$\dot{e}_2 = e_1 / T_G \qquad (5.4)$$

$$\dot{P}_m = \frac{2}{T_G}(e_2 - \dot{e}_2 \, T_W - P_m) \qquad (5.5)$$

$$\dot{e}_3 = \frac{1}{T_R}(\dot{e}_2 \, \delta T_R - e_3) \qquad (5.6)$$

## 5.2.3 DC Link Representation:

The DC current in the link is assumed to be equal to the current order which is the output of the dynamic system (power controller) shown in Fig.5.3. The input to the system are scheduled power $P_{ref}$ and scheduled DC system voltage $V_d$. The external control signal is derived from the AC system quantities which is given by the equation

$$ECS = \frac{A}{2\pi} (\Delta W) - B(\Delta \delta) \frac{180}{\pi} \qquad (5.7)$$

where   A -= is expressed in MW/Hz

B -   is expressed in MW/degree

$\Delta W$ -   incremental change in the difference in
speed of two machines

$\Delta \delta$  -   incremental change in the angular difference
of two machines.

From the Fig.5.3,

$$\dot{e}_4 = \frac{1}{T_R} \left( \frac{P_{ref}}{V_d} - e_4 \right) \qquad (5.8)$$

$$I_{dc} = e_4 + ECS \qquad (5.9)$$

where ECS is obtained from equation (5.7).

The DC system voltage $V_d$ is taken as the average
of the DC voltages at rectifier and inverter ends.  Thus

$$V_d = \frac{V_{dr} + V_{di}}{2} \qquad (5.10)$$

Hence the equations (5.7) to (5.10) describe the performance
of the power controller. Thus the DC current can be calculated
by the integration of the differential equation (5.8) which
is done along with the differential equations describing the
generator response.

The value of the DC current is  reflected on the
AC currents which are calculated as follows:

$$I_1 = \frac{3\sqrt{2}}{\pi} K_{1r} \, I_{dc} \qquad (5.11)$$

$$I_2 = \frac{3\sqrt{2}}{\pi} K_{1i} \, I_{dc} \qquad (5.12)$$

where $I_1$ is the AC current per pole on the rectifier side,

$I_2$ is the AC current per pole on the inverter side.

The effect of the DC link on the AC system is equivalent to having two nonlinear loads, one at the rectifier end and another at the inverter end. The power factor of these loads can be calculated from two different sets of equations which can be derived, corresponding to the two modes of operation (i) when the control is at rectifier end (ii) when the control is at inverter end. These equations are given below as per the reference 8 .

With current control at rectifier end:

The power factor at the inverter is given by the equation

$$Cos\emptyset_i = Cos\gamma[1 + (\frac{6I_{dc} K_{1i} X_{ci}}{\pi\sqrt{2} E_i})^2 + 2(\frac{6I_{dc} K_{1i} X_{ci}}{\pi\sqrt{2} E_i})Sin\emptyset_i]^{\frac{1}{2}}$$

$$- \frac{I_{dc} K_{1i} X_{ci}}{\sqrt{2} E_i} \qquad\qquad (5.13)$$

where $\emptyset_i$ is the power factor angle at the inverter end.

$E_i$ rms value of the of the inverter bus voltage.

$\gamma$ reference value of the extinction angle of the inverter.

$I_{dc}$ DC current.

$X_{ci}$ Commutating reactance for the inverter.

This equation has to be solved iteratively to determine the value of $Cos\emptyset_i$.

After calculating the value of $Cos\phi_i$, DC voltage at the inverter end is calculated from the equation

$$V_{di} = \frac{3\sqrt{2}}{\pi} K_{2i} E_i Cos\phi_i \qquad (5.14)$$

Then the DC voltage at the rectifier end $V_{dr}$ is calculated as

$$V_{dr} = V_{di} + R_{dc} I_{dc} \qquad (5.15)$$

where $R_{dc}$ is the DC line resistance.

The power factor at rectifier end can be calculated from the equation

$$Cos\phi_r = \frac{\pi V_{dr}}{3\sqrt{2} K_{2r} E_r} \qquad (5.16)$$

where $\phi_r$ - power factor angle at rectifier end,

$E_r$ - rms value of the rectifier bus voltage.

When current control is at inverter end:

The following equations which can be derived similarly as in set I are given below.

$$Cos\phi_r = Cos\,\alpha\,[1 + (\frac{6I_{dc} K_{1r} X_{cr}}{\sqrt{2} E_r})^2 + 2(\frac{6I_{dc} K_{1r} X_{cr}}{\sqrt{2} E_r})\,]^{\frac{1}{2}}$$

$$- \frac{I_{dc} K_{1r} X_{cr}}{\sqrt{2} E_r} \qquad (5.17)$$

where $\alpha$ = minimum firing angle of the rectifier

$$V_{dr} = \frac{3\sqrt{2}}{\pi} \, K_{2r} \, E_r \, Cos\emptyset_r \qquad (5.18)$$

where $Cos\emptyset_r$ is calculated from equation (5.19) which is solved iteratively.

With the knowledge of $V_{dr}$, $V_{di}$ can be calculated as

$$V_{di} = V_{dr} - R_{dc} \, I_{dc} \qquad (5.19)$$

the power factor at the inverter is calculated from the equation

$$Cos\emptyset_i = \frac{\pi \, V_{di}}{3 \, \sqrt{2} \, K_{2r} \, E_i} \qquad (5.20)$$

The real and rective powers at the rectifier end and at the inverter end are calculated from the following equations. They are required only at the instants when load balance on the AC system is carried out.

$$P_i = -E_i \, I_2 \, Cos\emptyset_i = \frac{K_{1i}}{K_{2i}} \, V_{di} \, I_{dc} \qquad (5.21)$$

$$Q_i = E_i \, I_2 \, Sin\emptyset_r \qquad (5.22)$$

$$P_r = E_r \, I_1 \, Cos\emptyset_r \qquad (5.23)$$

$$Q_r = E_r \, I_1 \, Sin\emptyset_r \qquad (5.24)$$

where $I_1$ and $I_2$ are obtained from eqn.(5.11) and (5.12). $Cos\emptyset_i$ and $Cos\emptyset_r$ are obtained from (5.13) and (5.16) or (5.17) and (5.20) depending on the mode of control operation. $Sin\emptyset_i$ and $Sin\emptyset_r$ can be calculated correspondingly and can be substituted in the above equations.

The constants introduced in the above set of equations enable the use of independent AC and DC system base quantities and have been explained in Chapter 3. However, to make the set of equations complete, they are again defined below.

$$K_{1r} = \frac{1}{\sqrt{3}} \frac{I_{db}}{I_{br}} \qquad (5.25)$$

$$K_{2r} = \frac{V_{br}}{V_{db}} \qquad (5.26)$$

$$K_{1i} = \frac{1}{\sqrt{3}} \frac{I_{db}}{I_{bi}} \qquad (5.27)$$

$$K_{2i} = \frac{V_{bi}}{V_{db}} \qquad (5.28)$$

where $V_{db}$ and $I_{db}$ are the base DC voltage per pole and base DC current per pole respectively.

$I_{br}$ and $I_{bi}$ are the base values of AC currents at the secondaries of rectifier and inverter transformers.

$V_{br}$ and $V_{bi}$ are the base values of the AC voltages at the secondaries of rectifier and inverter transformers.

5.2.4 Network Performance Equations:

The network algebraic equations are used for power flow calculations during the transient period. Using the bus admittance matrix $[Y_{Bus}]$, the voltage equations are given by (5.29) and are solved by Gauss-Siedel iterative technique.

$$E_p = \frac{P_p - jQ_p}{E_p^*} L_p - \sum_{\substack{q=1 \\ q \neq p}}^{n} YL_{pq} E_q \quad [24] \quad (5.29)$$

$$p = 1, 2, \ldots, n$$

The term $\dfrac{P_p - jQ_p}{E_p^*}$ represents the load current at bus $p$

where $P_p$   -   real power at bus p,

      $Q_p$   -   reactive power at bus p,

      n   -   number of buses

      $L_p = 1/Y_{pp}$

      $YL_{pq} = Y_{pq} L_p$

where $Y_{pp}$ and $Y_{pq}$ are the elements of $Y_{Bus}$ matrix.

The solution of load flow equations in the AC network requires the knowledge of the load characteristics at every load bus. The effect of the DC link as stated earlier is equivalent to having two loads at the two valve buses, the loads being represented by current source model. The governing equations are (5.21) to (5.24). The characteristics of these loads are nonlinear in that the power factors of the loads are variable and have to be found by iteration.

## 5.3 FLOWCHART

Fig.5.4 shows the flowchart for the transient stability program.
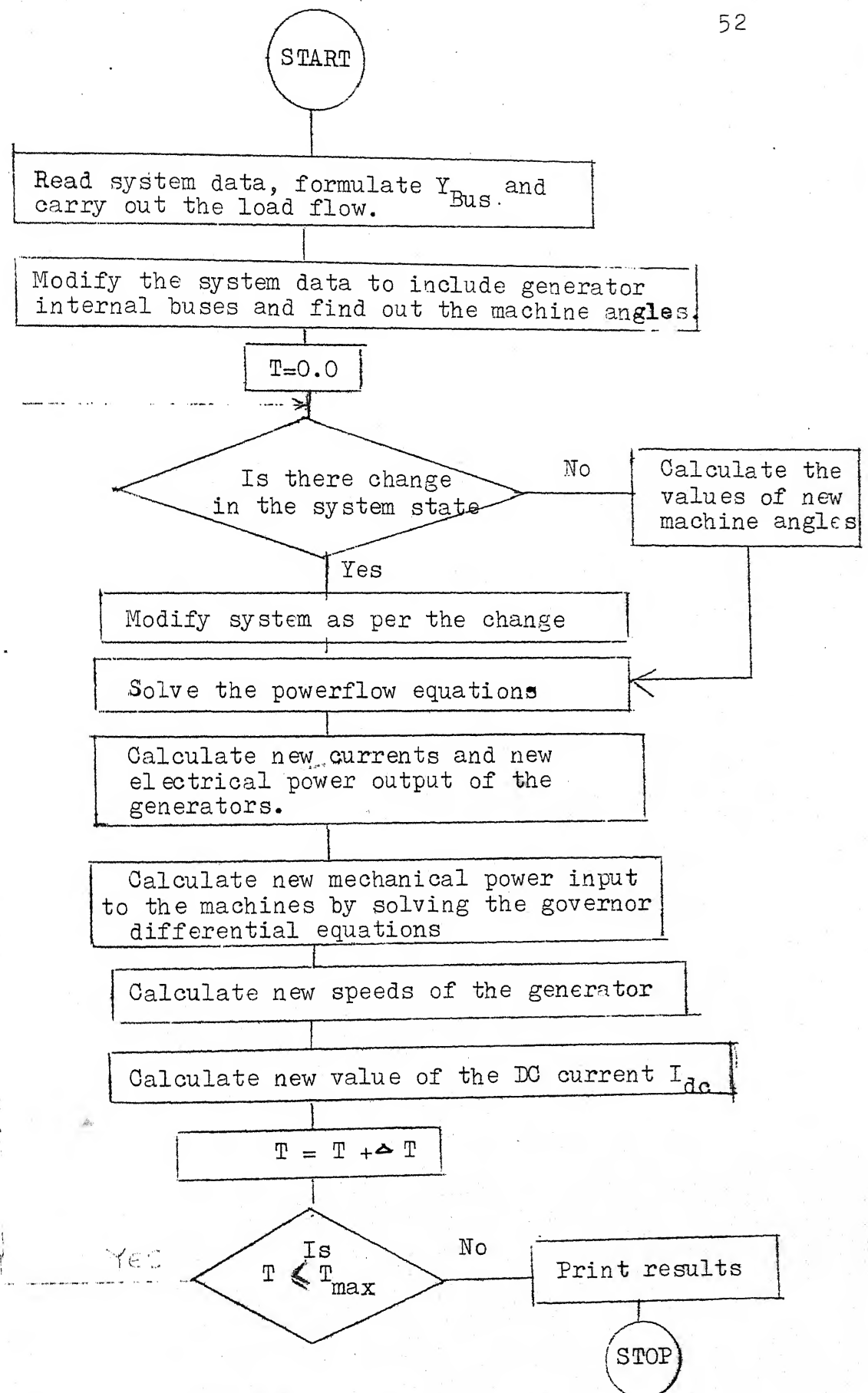
Fig. 5.4.

After reading system data and formulating the $Y_{Bus}$, the load flow is carried out. Then the system is modified to include the generator buses and the initial machine angles are determined. Then the simulation starts.

If there is any change in the state of the system, the system is modified accordingly. Otherwise, the new values of machine angle are obtained by solving the differential equation (5.1). Then the power flow equations are solved which are explained in the previous section. The new currents and electrical power output of the machines are calculated from the new system voltages obtained from load flow. By solving the governor differential equations (5.3) to (5.6) the new mechanical power input to the machines, are calculated. With the knowledge of the new electrical power input and mechanical power input of the machines, the new speeds and angles are determined by numerical integration. The updated value of the DC current is also calculated by numerical integration.

Then the time is incremented. If the time of simulation is not exceeded, the above procedure is repeated. The required results are printed at suitable intervals.

## 5.4 EXAMPLE

(i) <u>System data</u>: The system data considered is adapted from the paper by Uhlmann [17]

Generator data: Generating capacity of machine 1=1000 MW

Generating capacity of machine 2=1000 MW

Inertia constant (H) of machine 1 = 2

Inertia constant (H) of machine 2 = 4

Transient reactance ($X_d'$) for each

machine = $X_5 = X_6 = 0.3$

System nominal frequency (f) = 50.0

Local load at each generator bus

Real power = 500 MW

Reactive power = 250 MVAR

Transmission line reactances:

$X_3 = X_4 = 0.04$ p.u.

On 100 MVA base

$X_o = 0.2$ p.u.

DC line data:

Commutating reactance for rectifier = 0.08 p.u.

Commutating reactance for inverter = 0.08 p.u.

Minimum firing angle , $\alpha$ = 5°

Reference value of the extinction angle $\gamma = 60°$

Limits on the DC current

Lower limit = 0.1

Upper limit = 1.2

Time constant in the power controller $T_R = 0.35$ sec.

Constants for conversion into p.u. quantities:

$K_{1r} = K_{1i} = 0.43$

$K_{2r} = K_{2i} = 0.86$

Governor data:

Gate closing time $T_G$ = 5 sec.

Transient speed droop = 0.3

Damping time constant $T_R$ = 5 sec.

Water time constant $T_W$ = 1.5 sec.

Permanent speed droop = 0.05

(ii) Initial conditions:

$P_{dc}$ = 100 MW

$V_d$ = 1.0 p.u.

Slack bus (1) voltage = 1.0 + j0.0

$P_{AC}$ = 200 MW

Generator (2) output = 800 MW

5.5 RESULTS AND DISCUSSIONS

The following cases are studied to examine the transient stability of the system considered when one of the AC lines is permanently disconnected:

(a) without external control signal,

(b) with external control signal
with A = 100 MW/ Hz and B = 5.0 MW/degree

(c) with external control signal
with A = 750 MW/ Hz and B = 5.0 MW/degree

A and B being the constants used in eqn.(5.27).

The following groups are plotted.

(i) Relative machine angle $(\delta_2 - \delta_1)$ vs. time.

(ii) DC current $(I_{dc})$ versus time.

(a) Without external control signal:

As seen from the Fig.5.4(case a) the oscillations in the value of $\delta$ are increasing and thus the system is unstable. The reason for this is that no damping is provided by the DC system as the external control signal is absent.

(b) With external control signal:

With value of A = 100, and b =5.0.

From the Fig.5.4(case b) it can be observed that some damping is provided by the DC system. But still it is not sufficient to damp out the oscillations.

(c) With external control signal with value of A=750 and b = 5.0.

The possibility of modulating the power in the DC system to improve the system stability is clearly seen from Fig.5.4(case c). The rate of rise of DC current in highest in this case. The system is stable.

Thus it can be seen that the proper choice of the constants A and B is essential. The most important part of the control signal is A which introduces the damping into the system.

The results obtained here are similar to those presented by Uhlmann.

## 5.6 CONCLUSION

The mathematical modelling of the two machine
system having parallel AC/DC transmission lines has been
developed. The transient stbility programs has been
developed to obtain the response of the system on the
event of a disturbance.  Although the study is not
exhaustive it serves to illustrate the concepts of stabi-
lizing the AC system through an auxiliary controller in
the DC link.
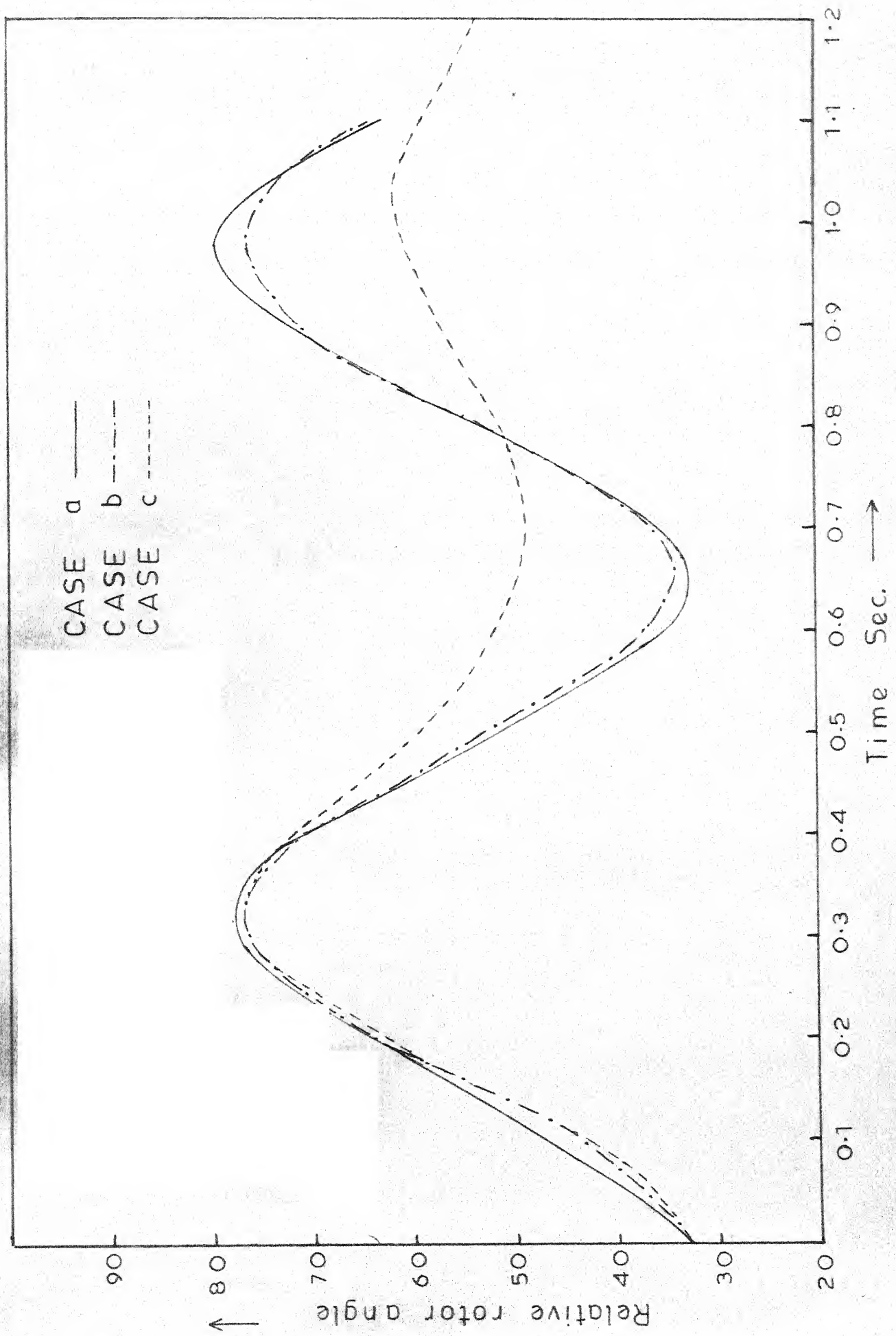
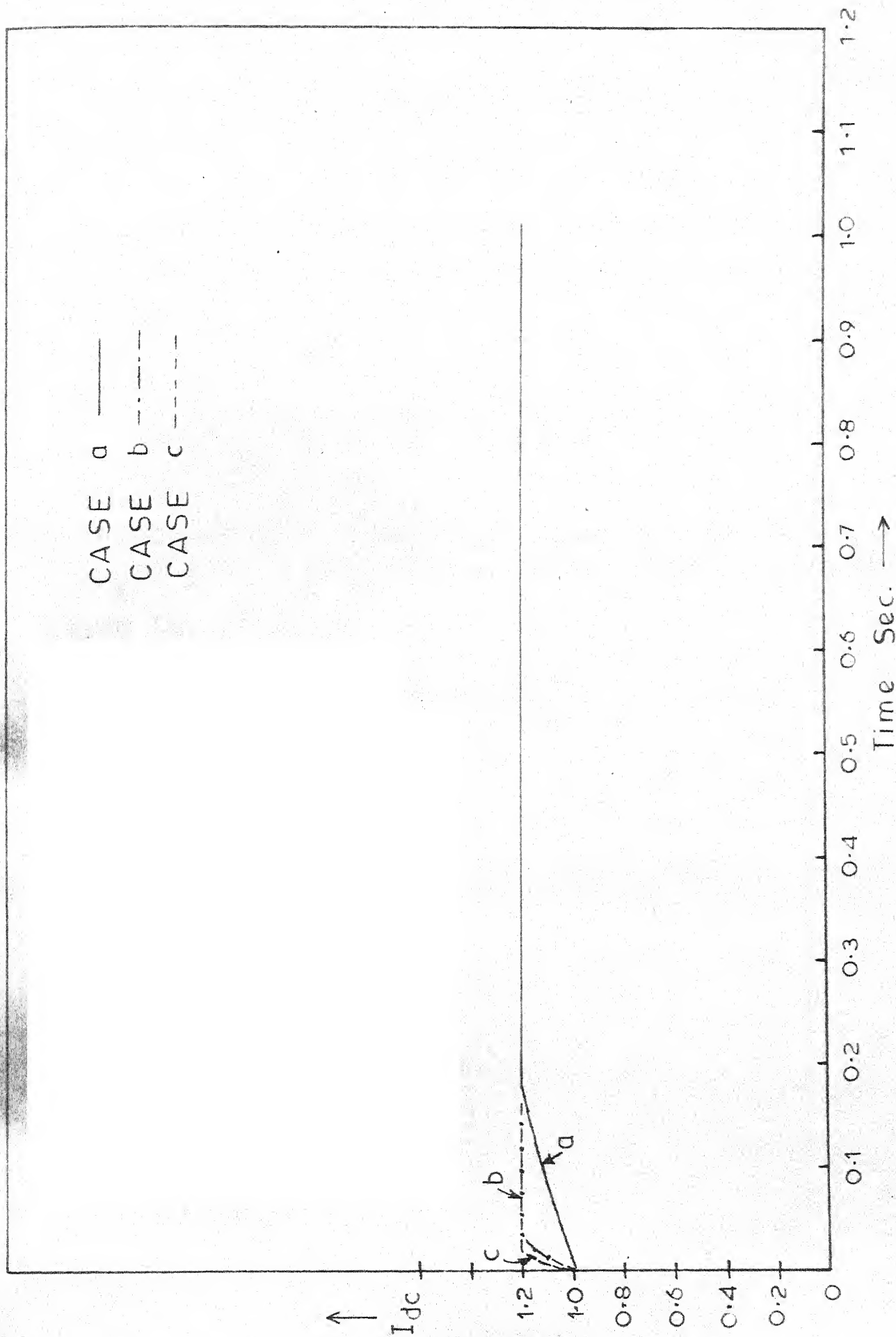FIG.5.4 RELATIVE ROTOR ANGLE ($\delta_2 - \delta_1$) VS TIME

58

FIG. 5.5 DC CURRENT ($I_{dc}$) VS TIME

# REFERENCES

1. Erich Uhlmann, Power Transmission by Direct Current, Berlin, Springer- Verlag, 1975.

2. John, J. Vithayathil, "Recent development in HVDC Transmission", presented in All India Conference on DC Technology, Feb. 1978.

3. E.W. Kimbark, Direct Current Transmission, Vol.1, Newyork, Wiley-Interscience, 1971.

4. M. Ramamoorty, An Introduction to Thyristors and Their Applications, New Delhi, Affliated East West Press, 1977.

5. F.G. Goodrich etal, "The use of high voltage direct current in the modern world - A brief review", presented in All India Conference on DC Technology, Feb. 1978,

6. Eckhard Rumpf, S. Ranade, "Comparison of control systems for HVDC Stations connected to weak AC systems, Part I-New control systems", IEEE, PAS, Vol.91, pp.549-555, March/April, 1972.

7. J.D. Ainsworth, "The phase locked oscillator, A new control system for controlled static converters", IEEE Trans. on PAS, vol.87, pp. 859-865.

8. W.K. Marshall, K.R. Padiyar, L.M. Denton, W.J.Smolinski and E.F. Hill, "A simplified HVDC link representation for system stability studies", Paper presented at IEEE Summer Power Meeting, July 1974.

9. E. Uhlmann, "Stabilization of an AC link by a parallel DC link", Direct Current, pp. 89-94, Aug.1964.

10. H.A. Peterson and P.C. Krause, Jr. "Damping of Power swings in a parallel AC and DC system ", IEEE Trans. on PAS, Vol.85, pp. 1231-1239, December 1966.

11. T. Machida, "Improving Transient Stability of AC system by joint usage of DC system", IEEE Trans. PAS, Vol.85, No.3, pp. 226-232, March 1966.

12. J. Kauferle and E. Rumpf, "The influence of HVDC Transmission system and their control on the stability of associated AC networks", CIGRE Report 32-15, 1970.

13. J.J. Dougherty and T. Hillesland, "Power system stability considerations with dynamically responsive DC transmission lines", IEEE Trans. PAS, Vol.89, pp. 34-45, Jan.1970.

14. M.S. Sachdev etal., "HVDC transmission link stability analysis by state space techniques", presented in Engineering Institute of Canada in 85th Annual general meeting, 1971.

15. M. Ramamoorty, etal., "Transient performance of a HVDC transmission system", IEEE Trans. PAS.

16. Peterson, etal., "Parallel operation of AC and DC power transmission", IEEE International Convention, 1964.

17. E. Uhlmann, "AC network stabilization by DC links", CIGRE Report, 32-01, 1970.

18. K.R. Padiyar, etal, "Stability studies on parallel AC and DC links", Proc.IEEE, Canadian Conference on Power and Communications, 1974.

19. J.W. Klein, "Parallel AC-DC systems, Dynamic stability assessment model", Trans. PAS, Vol.77, pp.1296-1304, July/Aug.1977.

20. W.A. Patterson etal, "More effective damping on AC systems through the addition of external control signals to a HVDC link, EEL River Case", Presented at Canadian Electrical Association in Spring meeting, March 1972.

21. W.A. Patterson, "External control system on the EEL River HVDC Scheme", Presented to Canadian conference on Automatic Control, Sept.1973.

22. R.L. Cresap and Mittlestadt, "Small signal modulation of the Pacific HVDC Intertie", IEEE Trans. on PAS, Vol.95, No.2, pp. 536-541, March/April 1976.

23. R.L. Cresap etal, "Operating experience with modulation of the Pacific HVDC intertie", Presented at IEEE PES Summer Meeting, July 1977.

24. Glen W.Stagg and Ahmed H.El-Abiad, Computer Methods in Power System Analysis, Tokyo, McGraw-Hill Kogakusha Ltd., 1968.